IEEE Journal of Microwaves

Received 10 May 2023; revised 3 June 2023; accepted 3 June 2023. Date of publication 28 June 2023; date of current version 7 July 2023.

Digital Object Identifier 10.1109/JMW.2023.3283395

Making Waves: Microwaves in Climate Change

RONNIE S. SIEGEL[1] AND PETER H. SIEGEL[2,3,4] (Life Fellow, IEEE)

(Special Series Paper)

[1]Swire Siegel Landscape Architects, La Canada, CA 91011 USA
[2]THz Global, La Canada, CA 91011 USA
[3]Department of Electrical Engineering, California Institute of Technology, Pasadena, CA 91125 USA
[4]NASA Jet Propulsion Laboratory, Pasadena, CA 91109 USA

CORRESPONDING AUTHOR: Peter H. Siegel (e-mail: phs@caltech.edu).

This work did not involve human subjects or animals in its research.

ABSTRACT Climate change is arguably the single most important global challenge of the 21st century. It is appropriate that in this, our first installment of our new editorial series *Making Waves*, we explore some of the ways that microwave technologies have been involved in this critical research field. Skipping over the obvious but essential roles of microwave communications and tracking in space-based resource management, we instead focus on techniques and data that these systems provide. We also look at some of the more unusual applications and ideas that are being enabled by both current and future microwave component advances and the impacts that they might have on local, and perhaps someday on more global scales. The intent of the article is to provide the reader with links between, and references to microwave technologies and climate science. The authors want to encourage more researchers to seek out and collaborate on ideas and proposals that directly or indirectly bridge these often disparate areas of development. They also look forward to responses from the engineering and science communities via this editorial series as a means of bringing together engineers and scientists interested in sharing new ideas and forging collaborations that might otherwise not form without such a stimulus. Future articles in this series will emphasize other potentially high impact fields with particular cross-over applications to microwave theory and technology.

INDEX TERMS Climate change, making waves, microwave remote sensing, microwave environmental applications, microwave radiometry, microwave radar, microwave power beaming, microwave heating, microwaves in fusion.

I. INTRODUCTION

Climate change is arguably the single most important global challenge of the 21st century. Energy consumption is rising rapidly, especially in developing countries, and the continued use of fossil fuels is bringing the world closer and closer to the brink of an irreversible climate catastrophe attributed to greenhouse gas production and its role in induced global temperature rise. There has never been a time when global resource and climate monitoring were more necessary, and when every direct or indirect method for reducing fossil fuel dependence and/or the release of additional greenhouse gases was essential. In this article we take a broad look at some of the microwave techniques that have traditionally played a major role in the field of resource management and in activities related to documenting and understanding climate change or mitigating its impacts.

Skipping over the obvious but essential roles of microwave communications and tracking in space-based[1] and ground-based wireless technologies and transportation management, we instead focus on techniques and data that these systems use and provide. We also survey some of the more unusual applications and ideas that are being enabled by both current and future microwave component and systems advances and

[1]Note that all satellites utilize radio frequency (generally microwave) uplinks and down links for control as well as data transmission back to earth. Although technically these applications of microwave signaling are at the very heart of all satellite (and most ground based communication and tracking) systems, we are purposely not including this as a science application involving climate change or global resource monitoring for this tutorial article. Rather we count this as enabling technology, since it is ubiquitous in almost every application where communications between a sensor and a data receiving station are involved, both on the ground and in airborne or space applications.

the impacts that they might have on processes that can assist in mitigating climate change. The intent of the article is to provide the reader with links and references to microwave technologies related to climate science, and to encourage more researchers to seek out and collaborate on ideas and proposals that directly or indirectly bridge these often disparate areas of development. The tutorial is broken up into sections that highlight particular characteristics and general applications of microwaves: sensing, heating, power generation, power beaming, and propagation.

We begin with the "elephant in the room" that is satellite systems that utilize microwave instruments and techniques to gather information on a global scale. These instruments help to assess and track various ground resources and atmospheric constituents over time, as well as furthering our understanding of processes and models that help shape climate policy. This is followed by a series of brief sojourns into applications where microwaves play some key role that may help mitigate our steadily advancing path towards global temperature rise, or coping with the consequences. These take the forms of reducing dependencies on fossil fuels; helping to reduce, transform, or capture emitted CO_2 or other catalytic chemicals; alternative or more efficient means of producing necessary chemicals or fuels; enhancing nutrients and crop yields; energy generation and transmission; and ways in which microwave measurements can help track and monitor enhanced weather related phenomena caused by global warming.

II. SATELLITE-BASED MICROWAVE SENSING

Satellite remote sensing spans almost the entire electromagnetic spectrum from the ultra violet to long radio waves. The particular wavelength range that is utilized depends on the specific function of the sensor (imaging and mapping, spectroscopy, tracking geophysical processes etc.), the desired resolution, and the transmission through the atmosphere (Fig. 1). The advantages of working in the microwave spectrum (1–300 GHz) are primarily: (1) the ability to penetrate through the atmosphere, even in the presence of clouds, rain, or dust; (2) emission and absorption features that are unique to this portion of the electromagnetic spectrum (vibrational and rotational spectral line transitions that can be used for fingerprinting particular gaseous molecules and atoms); (3) spectral radiance measurements that can be converted into accurate altitudinal-based temperature and pressure profiles on a global scale; (4) absolute ground and water temperatures; (5) 2D and 3D terrain mapping, emphasizing particular geological constituents, properties, or spectral signatures, including polarization (ice or snow, rock or vegetation, wet or dry soil, etc.); (6) highly accurate altimetry, even over water, and including snow and ice thickness and wave height; (7) wind and wave speeds and direction; and (8) the possibility for variable resolutions based on fixed and synthetic aperture antenna techniques.

Other remote sensing wavelengths and technologies can also perform some of these functions, and multi-spectral systems offer the most comprehensive measurement coverage. Many satellites carry a broad range of individual instruments

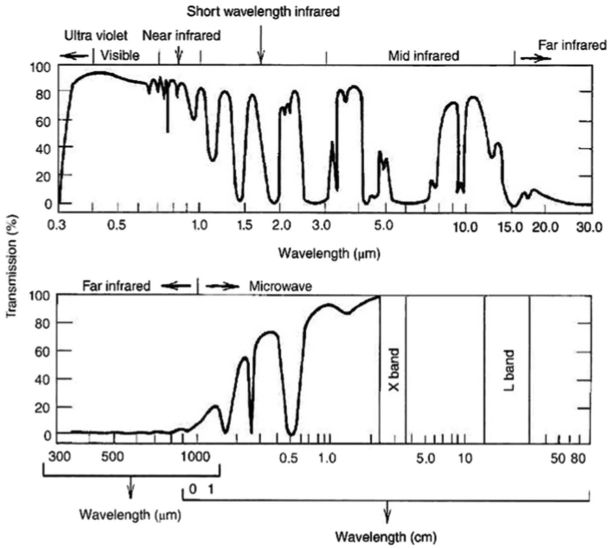

FIGURE 1. Transmission through the Earth's atmosphere from the UV through the radio spectrum. Copyright Charles Elachi, private communication 2023, with permission.

that cover wide swaths of the available remote sensing spectrum. These also have the advantage of cross correlating and cross calibrating distinct measurement products where data sets overlap. Since this is a microwave journal targeted at a microwave engineering audience, we will focus only on the microwave regime and the associated sensor systems that are most often being deployed and used.

Microwave remote sensing from space-borne and high altitude aircraft or balloon platforms is generally classified into two major categories: active sounding using radar techniques and passive sensing using radiometric methods.

Active microwave remote sensing has been at the forefront of the field of climate science since the development of *radar* (radio detection and ranging) and its very early use in measuring the height of the Earth's ionosphere at 4.28 MHz by Breit and Tuve in 1925 [1], [2].

Radar techniques employed on aircraft, balloon, or space-borne platforms are typically deployed for three common measurement categories: imaging, scattering (scatterometers), and ranging (altimeters). Within these categories information on object size, position, composition, distance, speed, and direction of motion are all possible. In addition, the resolution (for imaging purposes) can be either fixed by the actual transmitting/receiving antenna dimensions and the distance to the scene: $d = R\theta = R{*}1.22\lambda/D$, with d being the spot diameter, R the distance from the antenna or range, θ the antenna beamwidth, and D the antenna diameter, or it can be computationally enhanced in at least one dimension (along the satellite track, for example) using synthetic aperture techniques - increasing D by using the motion of the transmitter and coherently processing the signals from sequential pulses.

As the acronym implies, radar systems must generate and transmit a signal that is bounced, or scattered off the object being targeted and then detected after a generally known time delay (Fig. 2). The time delay is a function of the round trip

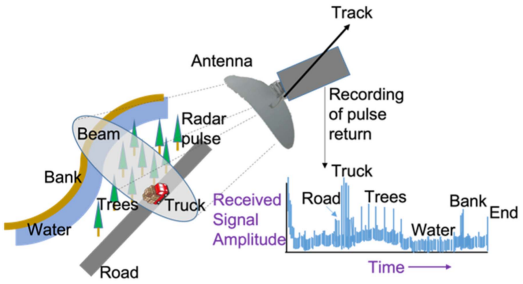

FIGURE 2. Cartoon of a typical satellite pulsed radar system imaging along a track and recording received backscattered energy from the illuminated scene over time. A single pulse retrieval is shown. Based on Fig. 1–16 in ref. [8].

distance to the target and back to the detector and yields the range through the velocity of radio wave propagation in the intervening media,[2] typically the velocity of light, c. In the simplest rendition the received power at the transmitting antenna over time $P_r(\mathrm{t})$, is related to the transmitted power P_t, by [4]: $P_r(t) = \alpha\ P_t\ (\mathrm{t} - \Delta\mathrm{t}) = \alpha\ P_t\ (\mathrm{t} - \frac{2R}{c})$, where R is the range, Δt is the round trip time, and α is a fraction that represents the very small amount of transmitted power that makes it back to the transceiver.

The transmitted power can be a continuous wave signal, a pulse, a frequency swept signal, an amplitude or phase modulated signal, or a combination, like a chirped pulse. The received signal will appear as a time delayed and modified version of the original transmitted wave and carries information about the scene itself or an object within the scene. If, as in almost all cases, the scene is large compared to a wavelength, return signals from different regions in the scene will arrive at different times due to differences in their ranges, and the above relationship becomes an integral over the various distances encountered [4]:

$$P_{\mathrm{r}}(\mathrm{t}) = \int \alpha\ \mathrm{P_t}\ \left(\mathrm{t} - \frac{2R}{c}\right)\ B(R)\ dR,$$

where $B(R)$ is the return from a series of small regions in the scene separated by a distance ΔR, and the integration limits involve the time of flight to all portions of the scene and the length of time the transmitted signal is deployed, typically the duration of the pulse, the modulation frequency sweep time, or the chirp period. From the point of view of power, when the transmit and receive antennas are the same, and have an effective area A, $\mathrm{P_r} = (\mathrm{P_t}A^2\sigma)/(4\pi\lambda^2R^4)$, where σ is the scattering cross section of the scene and is a function of the area, geometry, and material composition. This is the familiar radar equation for wavelengths much smaller than the scene, and shows that the power drops off as the distance to the fourth power. Note also that A^2 typically contains the antenna radius to the fourth power, so increasing antenna size has a dramatic effect on the return signal through the antenna gain. Again, in a satellite application where the scene is a large area s, and we are receiving signals from its individual parts, the received power is a sum over the area of the scene that the main antenna beam is illuminating [6]:

$$P_r = \frac{1}{4\pi\lambda^2} \int \frac{P_t A^2 \sigma^0}{R^4} ds,$$

where σ^0 is the average scattering coefficient across the scene.

For a continuous wave (CW) signal transmission of frequency f, radial motion in the scene towards or away from the source is directly translated into a frequency shift $f\pm\Delta$f through the Doppler effect and produces speed information [5]: velocity of an object in the scene, $v = c\Delta\mathrm{f}/(2f)$ for values much less than the speed of light.

With a pulsed radar, the amplitude variation of the return signal over the time window translates into information on the scattering properties of various points within the scene and can be used to construct images that reflect the characteristics of the individual objects within the field of view of a single pulsed waveform.

If a continuous wave transmitted signal is frequency modulated, for instance as a linear sawtooth-style sweep (FMCW), the received power spectrum can be converted to both range and amplitude. In this configuration the detected frequency sweep contains a frequency shift that relates directly to the distance [4]: $\Delta\mathrm{f} = K\Delta\mathrm{t} = 2KR/c$, with a range resolution of: $\Delta\mathrm{R} = c/(2B_w)$, where K is the slope of the linear frequency sweep, $(\Delta\mathrm{f}/\Delta\mathrm{t})$, and B_w is the bandwidth of the frequency sweep. This form of radar can be used for terrain mapping (3D imaging) as well as Doppler. The form of modulation can also be sinusoidal, square wave or keyed, a stepped staircase, triangular, or other variants to enhance specific object or scene parameters.

There are many dozens of excellent texts on various forms of radar techniques and instruments going back to the MIT Radiation Lab Series and series Editor Louis Ridenour's opening volume on Radar System Engineering [5]. For the most common satellite applications, where the distance to the scene is always much much greater than the antenna scale (focal length/diameter >> 1) the authors suggest the excellent series of three pioneering texts by Fawwaz Ulaby, et al. [4], [6], [7] from the 1980's, the single volume update by Ulaby and Long [8] in 2015, and the more recent text by Charles Elachi [9] and Jacob van Zyl, released in 2021 [10].

Passive microwave *radiometry* (extracting the equivalent temperature of an object by recording its electromagnetic power emission in the microwave frequency range) has been utilized for determining properties of the Earth since the invention of the "*Dicke-switched radiometer*" first described by renowned physicist and astronomer, Robert H. Dicke in 1946 [11]. The methodology uses a calibration load of known absolute blackbody temperature that is part of the same optical path, and observed via the same electronics detector package, that is employed for direct scene observations. The calibration source is sampled frequently enough, and over a long enough observation time, that random or systematic gain variations

[2]Note that in the microwave region the real part of the index of refraction of air is typically in the range of 1.0002 to 1.0006 [3] and is somewhat higher near the water vapor and oxygen absorption bands. The assumption of $v = c$ is therefore adequate for many purposes.

through the entire optical path (or at least out to the load position) are averaged out. In 1945, Dicke, and then MIT Radiation Lab colleagues R. Beringer, R. Kyhl and A. G. Vane, put the new methodology to good use in what is likely the first remote sensing and radiative transfer application in the microwave range: measuring atmospheric water vapor absorption at 20, 24, and 30 GHz using the background of cold space at different antenna tilt angles (varying atmospheric path lengths) with direct comparison to in-situ aircraft data [12].

In radiometric sounding the key measurement parameter is the brightness temperature of the object(s) in the observed scene comprising the beam area of the antenna on the ground as viewed through the distance to the receive antenna. The Rayleigh-Jeans approximation to Planck's Law (accurate to around 1% for wavelengths below 100 GHz and temperatures near 300 K) relates the brightness temperature of a perfect blackbody (material that absorbs all the radiation incident upon it) to its physical temperature T [13]: $B_{bb}(f) = 2kTf^2/c^2$ W/m^2/Hz/sr, where B_{bb} is the blackbody brightness temperature in frequency units, k is Boltzmann's constant, and f is the frequency.

The power that would be received by a perfect antenna immersed in a perfect blackbody emitter (or receiving a blackbody signal that fills the entire antenna beam) is simply [12], [14]: $P_r = kTB_w$, watts, where B_w is the bandwidth of the receiver in Hz. However, typical objects are not blackbodies and they absorb (or radiate) only a portion of the energy available from their physical surroundings. Their brightness temperature T_b can be expressed as the temperature at which a blackbody would produce the same power in the receiver: $T_b{=}\varepsilon T$, where ε is defined as the emissivity of the object or the average over the scene within the antenna beam. Perfect absorbers have an ε of 1, and perfect reflectors have an ε of 0. Emissivity is a function of the geometric and physical properties of an object (or scene) and varies with frequency and polarization as well as the surface roughness relative to a wavelength (scattering properties) and the direction of the received signal relative to the orientation of the antenna (tilt angle). Loosely quoting from [13], for frequencies around 10 GHz, sea water viewed directly from above has an emissivity of 0.37, loamy soil with 25 percent moisture content comes in at 0.6, and dry soil at 0.9. The corresponding brightness temperatures (assuming a physical temperature of 300 K for all three terrains) would then be [13] 111 K, 180 K, and 270 K, respectively.

When a real antenna is looking at a scene through a directed beam and an intervening medium, the brightness temperature emitted from the scene has to be processed through the loss of the medium, and extracted from the additional signals coming from (a) the medium itself (Earth's atmosphere, in this case), (b) directions other than those the primary antenna beam is pointing towards (pick up from back lobes and sidelobes), (c) reflections from the sky bouncing off the scene and entering the antenna via the main beam and also modified by the intervening medium, and (d) the antenna temperature itself

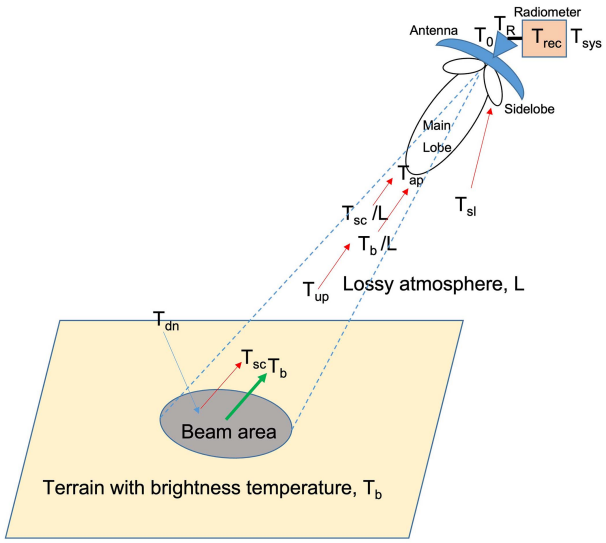

FIGURE 3. Terms in the radiometric signal reaching the antenna from the scene. Based on Fig. 1 in ref. [13].

(Fig. 3). Somewhat abridging [13]:

$$T_R = \eta\alpha T_{ap} + \eta\,(1-\alpha)\,T_{sl} + (1-\eta)\,T_0, \text{ with}$$

$$T_{ap} = \frac{1}{L}\,(T_b + T_{sc}) + T_{up}.$$

Here, T_R is the signal received at the antenna from a particular direction and with a particular footprint determined by the beam width and distance. T_b is contained within the T_{ap} term and is the actual brightness temperature we want to determine and record. η represents the antenna radiation efficiency (how much power goes into all the beams vs. what might be reflected or lost), and α represents the ratio of power in the main beam versus the side and back lobes. T_{ap} contains the scene brightness temperature we are trying to measure reduced by the loss L of the intervening atmosphere T_b/L, plus the reflected sky temperature T_{sc}, also reduced by L. T_{up} is the combined temperature of the atmosphere below the antenna (spacecraft) which also enters the main beam. T_{sl} is the received signal that enters through the sidelobes and back lobes of the antenna, and T_0 is the contribution of the antenna itself, assuming it is not a perfect receiver.

To make matters even more complex the loss in the atmosphere L, is a strong function of the frequency because many gaseous molecules are prevailing absorbers in the microwave region. Polar molecules such as water and oxygen are particularly problematic with dominant pressure broadened rotational transitions at 22.3, 183.3 and 323.8 GHz (water vapor), and 60 and 118.7 GHz (oxygen). These absorption resonances and others are in fact primary radiometer products for monitoring atmospheric processes and extracting vertical temperature and pressure profiles – oxygen is especially useful because it is well mixed in the atmosphere [14]. In order to accurately characterize the atmospheric path loss at different frequencies and across varying weather and cloud

conditions complex radiative transfer models are required and these have been given a lot of attention in the atmospheric science community [8], [10], [14].

Since thermal measurements of the Earth typically involve a temperature range between 3 K (cold space) and 320 K (ground) the temperature sensitivity (minimum detectable temperature difference) is a key performance metric of a radiometric receiver. Typically, heterodyne receiver systems are utilized with customized intermediate frequency bandwidth B_{IF} and integration time τ, and the minimum detectable temperature is [15]:

$$\Delta T_{\min} = T_{sys}/\sqrt{B_{IF}\tau},$$

where T_{sys} is the equivalent system noise temperature and includes contributions from the receiver, the antenna, and the scene. $\Delta T_{\min}$ can generally be arranged to be 1K or less for integration times shorter than a second and bandwidths in the MHz region using room temperature heterodyne receivers operating anywhere in the range from 1 to 300 GHz.

Unlike active radar remote sensing instruments, passive radiometers have more limited operating modes and somewhat less applicability. However, they are essential for making direct measurements of specific atmospheric constituents via the recording of unique spectral absorption/emission signatures (spectral lines) associated with the calculable quantum mechanical vibrational and rotational motions of polar molecules. Radiometers can also be used for imaging temperature variations in a scene associated with the brightness temperature difference within an observed terrain of mixed materials (i.e., water, soil, vegetation etc.). Most importantly, by utilizing accurate models for spectral line broadening by pressure and temperature, radiometers can measure these parameters (T and p) at altitude with well sampled vertical profiling, either from the ground or from space. Finally, by scanning through the atmosphere from an orbiting platform against the background of cold space, rather than aiming down towards the ground (the technique known as atmospheric limb scanning), direct measurements of the distribution and abundance of dozens of molecules comprising the stratosphere and upper troposphere can be measured across the globe on a daily basis providing essential data on water vapor, oxygen, carbon monoxide, sulfur dioxide, hydrochloric acid, OH, and many other gases associated with important global processes, including ozone depletion, acidification, and global warming [16].

In surveying the uses of these two techniques for the many hundreds of subsequent global studies related to climate change, we begin with some applications for satellite-based microwave radiometry and then follow with the more versatile active radar systems.

A. SATELLITE-BASED RADIOMETRY

The first successful satellite-borne microwave radiometer was flown on NASA's Mariner–2 spacecraft in 1962. The two channel radiometer operating at 15.8 and 22.2 GHz, and based on Dicke's pioneering load-switched microwave measurement techniques [11], returned early observations of the temperature of the Venusian atmosphere. Results showed that the atmosphere was optically thick (the microwave signals did not penetrate to the surface) and the atmosphere had an average temperature of around 500 K. The microwave instrument was developed at the NASA Jet Propulsion Laboratory by former mentor and dear friend, Frank Barath and his colleagues [17], [18] and was the start of the microwave remote sensing revolution that would help change the way we monitor our global environment.

The first use of radiometry for Earth observations from space came in 1968, with the launch of the USSR's Cosmos 243 [19]. The satellite carried four radiometers covering 3.5 to 37 GHz and measured water vapor, including cloud content, ocean surface temperature, sea ice borders surrounding Antarctica, and brightness temperatures on the ground and on sea water and ice. The US responded with two types of microwave radiometers on Nimbus 5 launched in 1972 and spearheaded by another former mentor and dear colleague at JPL – Joe W. Waters [20], who would go on to pioneer the use of microwave limb scanning up to THz frequencies [21]. The Nimbus E microwave spectrometer contained five nadir pointing radiometers covering the 22.2 GHz water vapor line for measuring humidity and cloud water content, and extended up to 58.8 GHz to cover the oxygen bands for deducing temperature profiles [22]. The temperature measurements agreed almost perfectly with in-situ balloon-borne radiosonde data [23] and established this technique as a principal method for long-term microwave observations of the atmospheric temperature from space. Nimbus 5 also carried an electronically steered array at 19 GHz to measure ground emissivity, and record snow and ice coverage.

By 1980, only eight years after Nimbus 5, more than a dozen satellite instruments had been deployed for Earth remote sensing observations using microwave radiometers [8]. In the past four decades this number has increased dramatically, as have the numbers of receiver channels, the frequency range, and the sensitivity (minimum detectable temperature differences). The development and deployment of the scanning multichannel microwave radiometer (SMMR) [24] on both Nimbus 7 and Seasat, both launched in 1978, set the stage for a series of core climatological measurement instruments that have flown continuously to this day, and are planned to fly well into the future. SMMR carried five radiometer channels from 6.6 to 37 GHz, but subsequent missions quickly increased the frequency to the 183 GHz water vapor line, with the advantage of much higher spatial resolution from the same size antenna. A parallel program in the US Air Force – DMSP (Defense Meteorological Satellite Program) launched a similar instrument - SSM/T (Special Sensor Microwave Temperature sounder) around the same time, with a 50-60 GHz receiver complement targeting oxygen, that also began a continuous measurement capability for meteorological and climate data monitoring for the military [25], [26].

Today substantially evolved versions of these instruments are being flown by the US National Oceanic and Atmospheric Administration (NOAA) under the designation JPSS (Joint Polar Satellite System) [27] and by the US Air Force Space

Command under the Defense Weather Satellite System [28]. Much of the data generated from the early instruments just enumerated have been recently reprocessed and are available in user friendly form on NASA's EARTHDATA web pages [29]. There are also many other countries that have since fielded passive microwave sounders for both meteorological and climate monitoring purposes including (the top six): Russia, China, U.K., Japan, India, and the European Union. More recently, commercial companies have gotten involved [30], and the push for smaller and less expensive platforms like CubeSat [31] have dramatically expanded the available suite of satellites fielding radiometric instruments.

The passive microwave sounders are mainly targeted at extremely accurate temperature profiling – day and night, in rain or fog, through clouds and dust. Beginning with the deployment of SMMR on Seasat, radiometric instruments have added measurements of [10]: water content in clouds, rain rates, wind velocity, sea temperature, sea ice concentrations, snow cover, and even soil moisture measurements using emissivity variations at different frequencies to extract surface or underground values [32]. As the retrieval algorithms improve, the data from passive microwave sounding gets better and better, and the half century of global monitoring data is now an essential constituent of the Earth's climate record [33].

Before leaving passive instruments it is worth mentioning one more style of microwave remote sensing that has had, and is still having, a very significant impact on climate monitoring, as well as in understanding important environmentally destructive processes such as ozone depletion [34]. This is the observing technique we mentioned earlier known as microwave limb scanning. Rather than looking down at the Earth, the satellite antenna scans through the atmospheric limb as it traverses its orbital path, nodding from the top of the stratosphere down to the troposphere, and collecting the emission spectra from discrete molecular line transitions as a function of altitude and position. By observing the thermal emission against cold space and arranging the antenna beam so that it collects data from a limited vertical profile beginning at the top of the atmosphere and dropping down in consistent steps, the spectral line signatures from each specific altitude within the beam path can be separated out. This results in a complete vertical and horizontal profile of the position and abundance of any of a large number of molecular species that can be continuously tracked and monitored. The technique was demonstrated with two major Earth remote sensing instruments developed at JPL under principal investigator Joe Waters: Upper Atmospheric Research Satellite Microwave Limb Sounder, launched in 1991, and Aura Microwave Limb Sounder launched in 2004 [21].

Although the infrared spectrum (1–15 microns) offers the most abundant radiometric dataset for current climate monitoring [35], microwave radiometric instruments have provided, and continue to provide, numerous climate relevant records. There are over 4200 references in Web of Science and 2000 on IEEEXplore that cover satellite microwave radiometers and applications including: water vapor profiling [36], [37], [38], surface and atmospheric temperature profiling [39], [40], [41], [42], [43], [44], [45], [46], rainfall [47], [48], [49], [50], soil moisture [51], [52], [53], vegetation coverage and land use [54], [55], snow cover and wetness [56], [57], [58], [59], water salinity [60], sea temperature [50], sea-ice [61], [62], [63], ground and water pollutants [64], [65], [66], ozone chemistry [34], [67], gases and pollutants in the atmosphere [16], [68], [69], [70], [71], ice and land mapping [46], [72], [73], cloud distribution and content [74], [75], [76], [77], [78], [79], ocean winds [80], [81], extreme weather [82], [83], [84], [85], [86], [87], volcanism [88], [89], [90], and many others , see Table 1-9 in ref. [8].

B. SATELLITE-BASED RADARS

Perhaps the first airborne radar microwave remote sensing measurement to look at atmospheric properties took place in the 1940s and consisted of a somewhat crude determination of the excess water vapor absorption on humid days from signals sent between two operational aircraft[3] [91], [92]. Rain radars based on particle-size-dependent backscattering soon emerged [93]. Synthetic aperture techniques were developed and demonstrated in the early 1960's [94], [95], [96]. NASA's Skylab, which launched in 1973, carried a 13.9 GHz pulsed radar altimeter which was primarily used for oceanographic sounding [97]. Ulaby and Moore [98] advocated combining radiometer and radar instruments to help with calibration, especially for ocean wind speed measurements made by radar scatterometers that correlated wave crests with velocity. By the time Charles Elachi and Walter Brown turned their L-band (1275 MHz) airborne synthetic aperture radar imager (designed for measuring snow and ice sheet thickness) towards the surface of the ocean in 1974 [99], remote sensing in the microwave regime was already well established. However, the new information – direct tracking of wave crests and subsequent retrieval of ocean wind speed– bought them an instrument slot on the upcoming NASA Seasat satellite program [9]. The extremely successful radar instrument deployment made microwave synthetic aperture radar a key component of many future space-based environmental monitoring platforms.

Seasat launched in June 1978, and along with the SAR instrument, carried a radar altimeter, a microwave scatterometer, and microwave radiometers for ocean and wave height, wind speed and direction, and emissivity and temperature, respectively. The 1275 MHz SAR radar used a 10.7x2.2 meter antenna and could resolve 25 meters on the ground [100], Fig. 4. The SAR system also imaged dry land. The long wavelength deep penetrating microwaves made some amazing pictures of subsurface features [101], as well as traversing through foliage covered regions and yielding a wide range of new geologic and environmental data that would play a

[3] J. H. van Fleck [91] and also Robert Dicke [12] both refer to some radar transmission and atmospheric sounding measurements made between aircraft flying in dry and humid air conditions and summarized in a 1944 MIT Radiation Laboratory Series technical report: R.S. Bender, A.E. Brent and J.W. Miller, "An aerial investigation of K-band radar performance under tropical atmospheric conditions," MIT Radiation Laboratory report 179, 1944. Available from: Barker Library Microfilms, FICHE TK6573.M41.A4 no. 729.

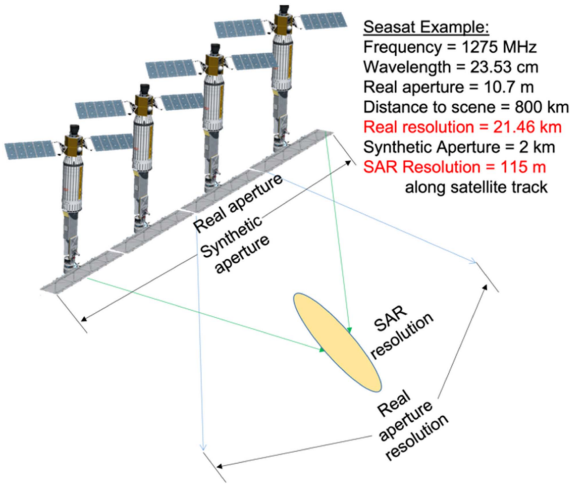

FIGURE 4. Example of resolution enhancement using SAR technique on Seasat.

significant role in resource management and human activities affecting the climate [102], [103]. Elachi and Brown also were able to use the SAR technique for rainfall monitoring [104] and many other valuable environmental applications [105], including 3D terrain mapping [106]. The SAR system flew on three additional NASA Shuttle missions and two major planetary missions (Magellan and Cassini), while Elachi was still involved. The technique continues to evolve and expand an already significant suite of applicable measurements. Many US SAR instruments, plus SAR systems from the European Space Agency, Japan, Germany, Canada, and even Argentina and Finland, have all been launched since Seasat [10].

Radar scatterometers have also played a significant role in Earth monitoring and mapping, and have accompanied SAR systems on many satellite platforms. Scatterometers are excellent at measuring wind speeds [85], [107], precipitation [108], cloud density [109], surface roughness and foliage coverage [110], [111], as well as other geologic features.

There are over 4200 references in Web of Science and 3200 on IEEEXplore that cover satellite microwave radar and applications including: cartography [112], mapping of urban spaces [113], monitoring of agricultural products [114], [115], [116], [117], [118], flood and drought monitoring [119], forest coverage [120], [121], [122], including fire risk [123], [124], [125], ice on lakes [126] and coastlines [127], [128], [129], as well as icebergs [130], snow cover [131], [132], oil spills [133], [134], soil moisture [135], [136], [137], [138], glacier mapping [139], and even undersea terrain mapping [140].

One last recent remote sensing innovation that has gotten a lot of attention is NASA JPL's Grace (gravity recovery and climate experiment) and its follow-on mission Grace-FO, launched in 2002 and 2018 respectively. The Grace platforms detect very subtle changes in gravitational pull on two synchronously orbiting satellites, originating from localized mass changes that occur directly below the orbital path. The differential gravitational pull affects the speed and position of one satellite relative to the other, and this very small change is monitored and recorded by 24 and 32 GHz radar ranging instruments that are accurate to ten microns [141]! Surprisingly, these minute motion shifts can be correlated with small mass changes under the satellites and can be used to very accurately track changes due to climate affected water reservoirs, underground water aquifers, glaciers, ice and snow pack, deep ocean pressure and height, and other relevant geological variables impacted by a changing climate.

New microwave radar applications include higher frequency instruments [142] that can measure water vapor profiles, cloud density and structure, and derive radiance and pressure profiles in the atmosphere with smaller antennas. The use of active interferometric techniques are now being deployed to get unprecedented resolution [143] without the need to have massive antennas or continuous synthetic aperture superposition.

C. ATMOSPHERIC SENSING WITHOUT SATELLITES

Many of the measurements that satellites can make with microwave radiometers and radars can generally be done from the ground with higher resolution (shorter range, and therefore smaller beam diameter), but more limited spatial coverage. Molecular line spectroscopy is one exception because the absorption in the lower atmosphere obscures the signals that are emitted higher up and pressure broadening obscures the fingerprinting available from individual emission signatures. For these measurements high altitude aircraft or balloon platforms are needed.

Ground based and airborne platforms often provide direct comparison with in-situ sampling to assist in calibrating remote sensing instrument products. NASA and NOAA in the US, and government agencies in many other countries as well, support a wide range of platforms and continuous campaigns for monitoring particular climate relevant atmospheric and geologic parameters [144]. These platforms (NASA has more than a dozen aircraft and over fifty specific ongoing science and observation programs [145]) provide the infrastructure to test new measurement techniques and technologies as well as to hone particular global change models or understand particular processes. The formation of hurricanes and cyclones, the distribution of clouds and aerosols, ice and snow coverage, water resource management, the impacts of wildfires, ozone levels, CO_2 studies, the convection of water vapor from the tropics into other latitudes, soil moisture and biomass studies, and many more climate related activities are being monitored [145]. The number of technical papers covering these microwave-based measurements and instruments is also voluminous: 7200 radar and 2150 radiometry remote sensing papers in Web of Science at last look, and 13,600 listings on IEEEXplore. It is not feasible to mention more than a few of these in this short tutorial.

Ground based radar has been used extensively for weather and climate monitoring since the 1940s when it was deployed to track free floating airborne radiosonde instruments in order to provide location information for in-situ weather measurements [146]. Extensive radar (and radiometer) observations were applied to the oceans (mostly from aircraft) in the 1960s [147]. Ocean temperature and surface roughness

were key parameters. By the 1970s, airborne and ground based radar systems were being deployed for geological and geomorphological measurements [148], snow and ice coverage, thickness, and water content [149], land surface roughness and wind speeds [150], soil moisture and vegetation coverage [151], and rain and weather monitoring [152]. The 1980s saw the rise of synthetic aperture techniques – both SAR and inverse SAR, and increased use of polarization information [153]. Ubiquitous Doppler radars measured local cloud cover and rain content [154], and uniquely identified clear air turbulence [155]. SAR interferometry and high resolution measurements were introduced in the 1980s [156]. From the 1990s onwards, the radar remote sensing field simply exploded with greatly improved retrieval algorithms, hundreds of new instruments, and a massive effort to increase existing, as well as to add, new resource monitoring programs, both to support climate science and the greatly increased satellite data that was pouring in [8]. Today, non-satellite based radar remote sensing goes from MHz [157] to THz [157], [159], and from monitoring birds [160], to finding deep underground coal fires [161], to locating plastic accumulations on the ocean [162].

On the radiometric front, ground based observations of the atmosphere to retrieve temperature and humidity profiles, based on the techniques of Dicke [12] and the calculations of van Vleck [91], have been ongoing since the 1950s [14], [163]. Aircraft and supporting ground measurements helped Ulaby et al. add passive emissivity characterizations for distinguishing soil moisture [164] and monitoring vegetation [165]. Staelin used radiometric imaging from aircraft for atmospheric profiling [166], and rain and storm monitoring [167]. Joe Waters [16] added molecular and atomic emission line measurements [168] reaching well into the THz spectrum [169] with his limb scanning technique from aircraft and balloon platforms [170]. High resolution ground terrain mapping in fog and through clouds was demonstrated by JPL's Bill Wilson in the 1980s using a first-of-its-kind helicopter-borne 98 GHz imaging radiometer [172]. Wilson also pioneered a passive radiometric wind sounder for aircraft measurements over the ocean [173]. Accurate snow and ice retrievals were developed in the 1990s [174], [175]. Today, ground-based microwave radiometers in a range of frequencies are actively deployed around the world for atmospheric monitoring [176], [177] and for local weather events [178], [179].

III. MICROWAVE HEATING

We now turn away from microwave radiometry and radar *sensing* techniques to take a look at a much more familiar characteristic of this region of the electromagnetic spectrum: *microwave heating*, and how this feature might be deployed in climate change studies or mitigation.

Using microwaves for heating foods and other substances – including people [180] – has been a widespread application since the realization of high power microwave resonance tubes (klystrons and magnetrons) in the 1920s [181] and 1930s [182]. Progress was enhanced after the design and successful commercial production of the microwave multiple-cavity magnetron by British physicists Sir John Randall and Henry Boot during World War II [183]. The magnetron was originally developed as a radar transmitter, but was soon commercialized for the food industry when Raytheon's Percy Spencer and Tappan appliances came together in the early 1960s to introduce the Radarange™ [184]. By 1967, the Amana Radarange was available for the homeowner for less than $500, and boasted kW output power in the microwave ISM (industrial, science and medical) bands at 914 MHz at 2.45 GHz [185].

Quoting from [186], "RF heating is based on the complex permittivity [185]: $\hat{\varepsilon} = \varepsilon_0\,(\varepsilon_r + j\varepsilon_i\,)$, where ε_0 is the free space permittivity in Farads/meter, ε_r is the real part of the dielectric constant, and $\varepsilon_i = \sigma/\omega\varepsilon_0$ is the imaginary part, with σ the conductivity in Siemens/meter and $\omega = 2\pi f$ the applied frequency. The RF absorption comes from σ via excitation of free carriers or electric polarizability (dipole absorption) and is conveniently expressed by the ratio of $\varepsilon_i/\varepsilon_r \equiv \tan\delta = \sigma/(\omega\varepsilon_0\varepsilon_r)$. The power dissipated, or the heating of the material at a given internal location, is then given by $P_i(x, y, z) = \sigma|E_i(x, y, z)|^2 = \omega\varepsilon_0\varepsilon_r \tan\,\delta|E_i|^2$, where E_i is the field inside [185]. For a sample that is small compared to the wavelength there is very inefficient power absorption. When the sample is on the order of the wavelength there can be significant or even resonant absorption, and when the sample is large compared to the wavelength there will be an exponential penetration of the power $P_{inside} = P_{surface}e^{-\alpha x}$, where x is the depth in cm, and α is the absorption coefficient in cm^{-1}. The field drops to $1/e$ of its surface value at a depth D, [185]:

$$D = (0.225\lambda_0)/\left\{\sqrt{\varepsilon_r}\sqrt{\sqrt{(1+tan^2\delta)}-1}\;\right\},$$

where λ_0 is the wavelength in free space. When $\tan\,\delta << 1$, $D \approx 0.318\lambda_0/(\sqrt{\varepsilon_r}\tan\delta)$."

For gases at low pressure, the microwave excitation goes directly into resonant absorption modes (rotational and vibrational motions) that characterize, and are unique to, particular polar molecules, and the energy can cause both heating and mode changes. Water vapor is the most ubiquitous target, and hydrolysis to generate hydrogen gas, the most obvious climate-aligned energy application.

Today, the magnetron and its higher power electron streaming succedents (gyrotrons and orbitrons) are still the most efficient way to generate high power microwaves, despite the recent development of high power solid-state semiconductor materials and amplifiers[4] [187]. Even in the 1960s, power levels in the kilowatt range could be generated with fist-sized components and efficiencies approaching 80% [188]. Scaling up in power to the gigawatt range [189] or in frequency to the THz regime [190] appear feasible. This has opened up a range of potential heating applications that can have both a direct (through replacement of fossil fuel

[4]914 and 2540 MHz magnetrons in commercial microwave ovens have advertised efficiencies (plug-to-RF) between 70 and 88% at power levels approaching 1kW. New GaN and SiC power amps are getting closer with power added efficiencies of over 60% at these frequencies and similar power levels, at least at 914 MHz [187].

sources), and a peripheral (through chemical processes) impact on climate change. We examine a few of these connections and potential applications next.

A. DRYING

The drying of materials and foodstuffs is as old a technology as one might imagine, and involves every conceivable form of heat transfer from direct burning of wood, to wind and solar, to modern electrical induction. From the point of view of energy efficiency (total kW hours needed to evaporate 1 kg of water from a material) microwave heating falls into the middle of the pack of available non-fossil fuel burning drying solutions with a typical value of 5 kWh/kg and efficiencies ranging wildly from 8 to 62% [191]. There is a strong dependence on the dielectric properties of the material being heated, the physical arrangement, and the coupling efficiency of the RF, which is frequency, mode, and geometry dependent.

Induction, solar, and vacuum drying are all somewhat more efficient than microwave techniques [191], but each has its limitations. For particular applications, such as food and grain drying via a fluidized bed (hot air levitating particulates in a sealed chamber), microwave assisted heating improves the efficiency by 95% over hot air alone [192]. In pyrolysis, heating is done in the absence of oxygen and leads to irreversible chemical decomposition. Gaseous, liquid, and solid products are all possible. Microwaves are used in speeding up the reactions, increasing the heating efficiency, and maintaining lower pyrolysis temperatures (in the range of 200–300 C) [193].

Other microwave and microwave-assisted heating applications are widespread and include everything from clothes dryers [194] to leaf (herb and tea) drying [195], and plant-based human and animal food preservation [196]. Industrial waste pre-processing is also a common microwave application [197]. There is even some research involving positive impacts of microwave heating on enhancing plant nutrition [198], vegetable disease mitigation [199], and extraction of pollutants [200].

Microwave heating based on current RF source technology is a fairly efficient electrical technique and avoids the use of direct fossil fuel consumption. For most applications (including those described in the next several sections), one can visualize the source as a form of microwave oven consisting of a magnetron and a cavity (or waveguide) containing the material to be heated. For heating gases, a sealed chamber can be used. As mentioned earlier there is also a growing potential for the use of all solid-state sources with high efficiencies [187], [201].

B. ALTERNATIVE FUEL PRODUCTION

Perhaps the most prolific use of microwave and microwave-assisted heating as related to climate change at the current time, is in the conversion of biomass (from deceased plants and animals), municipal solid waste (sewage), and industrial waste (plastics and oil) into sustainable fuels. There are literally dozens of pyrolysis and catalyst assisted processes being looked at, both in the laboratory and on an industrial scale, that utilize microwaves at one or more stages of the conversion process. For biomass, typically the end product is either ethanol (C_2H_5OH) or sometimes syngas (generally methanol CH_3OH); biodiesel (fatty acid esters with an alcohol group generated from vegetable oils and animal fats); or biogas (mostly methane CH_4 and carbon dioxide CO_2). The methane and CO_2 can also be further processed to make hydrogen gas H_2 and carbon monoxide CO. Another end product, biochar (charcoal composed of biomass products) is discussed in the next section. Typical heating temperatures are between 200 and 600 C depending on process and biomass material, but temperatures as high as 900 C are not uncommon for some processes.

Biomass production exceeds 120 billion tons per year worldwide (10 billion tons dry weight) with an energy capacity of around 2.2×10^{21} J [202]. According to United Nations statistics, the average global energy use in 2022 was approximately 6.2×10^{20} J [203], well below the potentially available biomass energy resources. However, biomass output must also provide the needed food for the world's population. Current output hovers around 10 billion tons of vegetable crops and 330 million tons of animal products, not yet sufficient to eliminate worldwide hunger [204]. This means the search for additional biomass sources is ongoing, and includes waste cotton [205], water cultivated algal sources [206], discarded animal fats [207], and other biowaste materials [208].

Making biofuels [209], [210] and other useful chemical commodities involves multiple steps and many intermediary products [202] too complex and numerous to go into here, but many of these require pyrolysis at some stage [211], [212]. Microwave heating offers the potential for deep penetration into the biomass material and effective temperature control. Microwave assisted pyrolysis also has rapid turn on and turn off, no requirement for agitation, and the potential for uniform internal heating, assuming the material has uniform volume dielectric properties. In this issue of IEEE JOURNAL OF MICROWAVES, Robinson et al. [201] show that single frequency solid-state microwave sources can allow for some input tuning and subsequent match into the biomass material for much higher coupling efficiency and much more efficient internal heating.

C. BIOCHAR

Biochar (Fig. 5) is an indispensable recycled material with an incredibly wide range of applications that relate directly and indirectly to climate change mitigation [213]. Biochar can be an end product of biomass pyrolysis and it can be an important fuel source in and of itself. Essentially it is solid carbon (charcoal) but produced from (amongst other treatments and catalysts) slow or fast heating of some initial biomass material in an anaerobic process. If derived from plants, it is often classified as carbon neutral because its production from biomass involves initial carbon capture through photosynthesis [202]. The biochar can also be used in the aforementioned fuel extraction process as an enhanced microwave absorber to increase the microwave coupling efficiency and speed up heating [214]. Biochar is also an extremely important ingredient for improving water retention in soils, filtering out noxious

FIGURE 5. Typical biochar product. From Giving Green.Earth , Jan 2023. (https://www.givinggreen.earth/carbon-offsets-research/biochar-%26-bio-oil).

chemicals, improving crop yield as part of a fertilization regimen, sequestering carbon for extended periods, and dealing with an ever increasing accumulation of solid waste [215].

The heat required to create biochar is between 300 and 900 C depending on the process used and the starting materials [214], Table I. As with most microwave heating applications, the ISM bands at 914 and 2450 MHz are typically employed. With a fast heating process (and higher temperatures – up to 900 C) more biochar is generally produced than in a slow pyrolysis reaction (temperature typically below 500 C) [214]. The particular choice of process depends on many factors including the production of associated gases (slow process) or bio-oil (fast pyrolysis). As with any carbonized product, the absorption properties of the material are also useful in a wide range of applications from water filtering to serving as a catalyst in a variety of chemical production processes. Besides its use as a heating agent (production value of 29-30 kJ/gm [193]), biochar is also a CO_2 sink and its ultimate composition can be controlled by appropriate choice of initial biomass properties [214]. It has been proposed as a carbon capture and cleansing agent for large scale agricultural use (as a fertilizer) and many other applications that can help ameliorate the impacts of climate change [213], [214], [215].

D. CHEMICAL CONVERSIONS

In a final application for microwave-assisted heating related to mitigating the impacts of climate change we take a brief look at gas conversion – both creating cleaner burning fuels and capturing or converting CO_2. Both of these chemical processes can be assisted with the application of microwave heating.

Converting CO_2 into other products involves breaking two highly stable covalent bonds (O=C=O) and generally requires significant energy. A promising technique is to use a non-thermal plasma discharge, and microwave sources can play a role in this process [216]. The microwave energy is generally delivered to the gas chamber through a waveguide using a high power pulse in the several hundred MHz to few GHz frequency range, or the gas can flow directly through the source waveguide. Many common CO_2 conversion reactions are possible but one of the most common is the production of ethanol (CH_3OH). A commercial system mentioned in [216] can produce 1.5 kilotons of ethanol per year from 3.3 kilotons of biomass.

Conversion of atmospheric CO_2 into solids or liquids for long term storage is also an application of interest, and microwave magnetrons can be efficiently employed for this process [217], [218]. Plasma temperatures can reach 6000 K and energy conversion efficiencies are reported to be between 40 and 90% [217], Table I. Finally, CO_2 char can be converted to CO ($C + CO_2 \leftrightarrow 2CO$) for gaseous fuel storage and reuse employing microwave heating (gasification) [219]. Extremely high efficiency can be achieved (97%) with gas temperatures in the 900 C range. H_2 can also be produced through: $H_2 + CO_2 \leftrightarrow CO + H_2O$ with excellent efficiency [219]. Other researchers have reported similar gasification advantages using microwave heating [220], and the conversion of CO_2 into many useful chemical products [217].

Other types of carbon conversions are possible with the introduction of catalysts and additional gaseous compounds, and many can benefit from the very efficient microwave assisted heating of polar gases at their resonant frequencies, or using broadly applicable microwave plasma discharge. Expansion of the technologies to large commercial scale plants is still a challenge, but our next topic involves the scaling up of microwave sources to enormously high output power. These may someday be applied to the carbon capture and carbon gasification processes just described.

IV. MICROWAVES IN FUSION

One of our best hopes for solving the energy production bottleneck has always been the potential to develop commercially viable fusion reactors. Despite the decades long (first controlled fusion reactor using magnetic confinement was Los Alamos National Laboratory's Scylla I in 1958 [221]) investment in this potentially infinite source of clean energy, there is still no solution in hand. However, there are many major research programs ongoing, and significant progress continues for both laser assisted (heated fuel pellet) and traditional tokamak style (magnetic torus plasma confinement) approaches. In the tokamak world microwaves play a key part in heating up the plasma. We expect to publish an excellent review and detailed description of the microwave techniques employed in the plasma fusion community in an upcoming article [222] from which we have generated the summary which follows.

Plasma temperatures for achieving the conditions for fusion are in excess of 150 million degrees. The strong toroidal magnetic field and the presence of a high density plasma causes electrons to spiral around the field lines in a path that resonates with a frequency that is determined by the strength and direction of the field, the electron cyclotron resonance ECR: $f_{ecr} = eB/(2\pi m_e)$, where e is the electron charge, B is the magnetic field, and m_e is the electron mass. For very high fields the electron mass has to be replaced by its relativistic form with the rest mass $m_{o,e}$ increased by the usual velocity modification: $1/\sqrt{1 - \frac{v^2}{c^2}}$. Since tokamak magnetic fields tend to be in the 1-10 Tesla range, the ECR frequency varies between a few GHz

to over 150 GHz. Sometimes both the fundamental and second harmonic ECR frequencies are targeted for plasma heating.

The required microwave power levels to produce the high temperatures required for fusion are typically in the several hundred kW to 10 MW range. The largest demonstration tokamak system now under construction, the International Thermonuclear Experimental Reactor (ITER) will use both inductive heating and heat generated by the fusion reaction itself for its primary source of energy. However, it will also deliver more than 20 megawatts of microwave power at 170 GHz to its magnetically confined plasma as an ECR assist to its primary heating system.

There are two other resonant frequencies that plasma scientists make use of for heating in their tokamak reactors, the ion cyclotron resonance (ICR) frequency, and the lower hybrid (LH) oscillation frequency. The ICR is similar to the ECR, but falls at a much lower frequency due to the higher mass of the ions in the plasma (typically protons) and is generally in the MHz region. The LH excitation is a longitudinal oscillation in the direction of the magnetic field and involves both electrons and ions. It falls in the middle of the ECR and ICR frequencies and is typically in the 2–10 GHz range. The LH mode is particularly useful for driving currents in the plasma that can get as high as 100 kA!

The microwave sources needed for generating the extremely high powers used in tokamaks (from MHz to >100 GHz) vary in design and implementation, and for the ICR mode, solid-state devices using GaN amplifier technology can satisfy some fusion programs. However, most fusion applications employ high power electron tube devices such as traveling wave tube amplifiers [223], klystrons [224], and gyrotrons [225] to excite the three common plasma heating modes.

Even though plasma heating can be demonstrated using pulsed microwave power, continuous wave operation is eventually required. The desired energy is so high that it usually requires several individual sources to be efficiently power combined, or at least synchronized to fall onto the plasma from multiple directions and locations. In the more powerful reactors such as ITER, twenty-four individual 1 MW gyrotrons with a pulse length greater than 500 seconds will be eventually employed for the ECR heating alone [222]!

V. MICROWAVE POWER BEAMING

One of the authors remembers with great interest reading William Brown's 1974 PROCEEDINGS OF THE IEEE article on microwave power beaming [226] while an undergraduate studying physics. Having had some fun as a secondary school student building and flying gasoline powered model airplanes, he was impressed both by the space-age properties of this invisible beam of guided energy, as well as its use in powering a model helicopter carrying a relatively quiet electric motor. (He was also influenced by Brown's more personalized writing style for technical publications)! Although he can't say that this article alone pushed him into electrical engineering, by the time Brown's MTT Transactions article on space-power beaming came out in 1992 [227], he was already fully entrenched in the microwave community.

At first glance, the idea of sending power through space, instead of high cost and generally more lossy transmission lines or waveguides, seems both extremely titillating, as it solves a major problem in energy distribution, and at the same time fatally flawed, because it necessarily carves out an invisible region in space through which objects cross at their own peril. The concept depends on the efficient conversion of electrical energy (DC or plug power) into microwave frequencies, very effective illumination and focusing of the microwave power into, and out of, a large antenna, and then collecting as much of the RF energy as possible at a specific distance, while simultaneously converting it back to DC using a rectenna (rectifying device embedded into a receiving antenna).

The issues of safety and electromagnetic interference aside, when applied to climate change, the power beaming concept serves two major purposes: (1) it allows efficient distribution of energy over large distances on the ground, so as to bring green energy from a distant or difficult to reach point of origin to the end users, and (2) it might possibly solve the intermittent solar energy generation problem (both weather related and lack of night time operation) if the solar panels were placed above the atmosphere and the power was beamed down to the ground. Both of these applications have recently been reviewed in three excellent papers from this journal by Chris Rodenbeck et al., [228], [229], and Naoki Shinohara [230]. We summarize a few of the more salient features from these papers here. Note that power beaming can also be accomplished with optical wavelengths but suffers much more from atmospheric propagation losses (rain, dust, and clouds) when employed for the two circumstances relevant to climate change described here.

In spite of what one might expect from the large number and span of the involved frequency conversions, the overall efficiency in going from DC to microwaves and back is actually not too terrible, with a record value of 54% set in the laboratory by William Brown himself in 1975 [227]. High power microwave tubes and solid-state power devices can have plug-to-RF efficiencies of 70-90% and rectifying antennas that directly convert the received RF to DC have demonstrated efficiencies of 85% or more [227]. If the frequency employed is below 10 GHz, the atmospheric attenuation is minimal over large distances, and only very modestly impacted by heavy rain or clouds, see Fig. 7 in ref. [228]. The most lossy portion of the link is the aperture-to-aperture coupling which, due to diffraction, follows a coupling metric τ that varies from 0 to approximately 2.5 for beam transmit and collection efficiencies spanning 0 to 100% [227], [228]:

$$\tau = \sqrt{A_T A_R}/(\lambda d),$$

where A_T and A_R are the transmit and receive aperture areas, λ is the wavelength and d is the separation of the two antennas. For small d, the antenna-to-antenna coupling efficiency can approach 100%, but for distances approximating far-field values: $2D^2/\lambda$, D being the antenna diameter, the efficiency is generally below 15% [228]. Note that at large distances, the receive aperture is typically much larger than the transmit aperture due to significant beam diffraction and the desire to

intercept as much transmitted power as possible. Surprisingly, the A_T to A_R coupling is strongest when the distance between the apertures falls into the Fresnel region (roughly $0.6\ D^2/\lambda < d < 2D^2/\lambda$), and when the transmitting aperture field distribution is optimized in amplitude and phase for the specific collection distance, see Fig. 6 in ref. [228].

The record for the highest received power over the longest path is from a test conducted at NASA's Goldstone antenna by Brown and JPL colleagues in the 1990s and stands at 35 kW over 1.55 km using a frequency of 2.4 GHz [228]. The issue of safety is dealt with by requiring that the power density anywhere within the propagating beam falls below the ICNIRP (International Commission on Non-Ionizing Radiation Protection) recommended limits for unrestricted full body exposure of RF below 6 GHz of 1 mW/cm^2 for 30 minutes [231]. For low microwave frequencies and large apertures this is a workable restriction, although some concepts for very high power systems seem to exceed this limit under conditions that the beam can be defocused, turned off, dimmed, or redirected, if breached by people, animals and birds, or reflective objects [228]. At least one large scale demonstration program to transmit 10 GHz power at km distances (1.1 km in this instance) was recently described by Rodenbeck et al. [229] and yielded 1.6 kW of received DC power with 91.2 kW transmitted (1.8% RF-DC efficiency), but projected improvements show efficiency gains up to 44%. Whether this technology can replace power transmission lines is still to be determined, but the potential for at least some niche uses seems plausible.

The second part of the power beaming dream is to collect solar energy continuously using an orbital platform and beam the power to the ground where it is picked up by an enormous rectifying antenna ground array and converted to DC. There is actually a NASA concept dubbed the Space Solar Power Satellite that was proposed in 1968 by Peter Glaser [232]. The initial design used a satellite in geosynchronous orbit (35,000 km from the Earth) with a solar array spanning 10 km^2! The proposal has undergone several iterations since, but at least two recent designs are still on the books and parameterized in [228]. One would work at 2.45 GHz and the other at 5.8 GHz (also an ISM band). Both would hope to provide gigawatts of DC power through a solar array that is four times more efficient in space than in the desert and bigger than Godzilla! The lower frequency concept transmits from a 1 km diameter antenna to a 10 km diameter ground rectenna array, while the higher frequency system requires only a half-km transmitter. Both concepts rely on an ambitious photovoltaic-to-ground DC conversion efficiency of close to 50%. Details can be found in [233], but don't count on implementation anytime soon.[5]

[5]In a post-review development, Caltech's Ali Hajimiri and team have successfully demonstrated the first wireless power beaming in space, between a transmit antenna and LED array, on the Space Solar Power Demonstrator (SSPD-1) satellite. The instrument, MAPLE (microwave array power-transfer low-orbit experiment), was launched on January 3, 2023 and is partly funded through a private foundation. A portion of the space-based power transmission was also detected on the ground using a radio telescope on the Caltech campus [234].

VI. MICROWAVE PROPAGATION AND OTHER IMPACTS

In this last short section, we mention a few interesting additional topics where microwaves and climate science intersect.

These days, we all depend so heavily on wireless communications that anything disrupting or influencing atmospheric propagation has widespread and significant consequences. As the climate changes, forecasts as well as demonstrated evidence for more severe weather events continue to amass. Kevin Paulson in Australia [235] and Péter Kántor and János Bitó in Hungary [236] have been examining the impact of severe weather, especially rainfall, on wireless links. This is certainly a topic that will rise in interest levels as storms increase in frequency and scale. There may be additional weather related variations in the quality and required density and power levels of our microwave communications networks as temperatures in some places increase, and atmospheric humidity levels continue to change.

Along the same vein, windshear is a nagging hazard for civilian and military aircraft and there is growing evidence that climate change is making things worse [237]. Both microwave Doppler radar [155], [238] and active microwave interferometry [239] can help. Microwave radar can also track bird migrations [160] which helps our understanding of both adaptation of species to climate change as well as global climate conditions. There are other localized weather events and patterns from tracking snow and hail, to severe winds in cyclones and hurricanes, and quantifying atmospheric water vapor during droughts, that are all aided by microwave techniques that have been mentioned in prior sections, but that will become more important as the climate evolves.

Turning to even more exotic couplings between climate and microwaves, we could not pass up the article by Takashi Ohira of Toyohashi University of Technology in Japan who wants to change the way we intend to use our electric vehicle technology by adding high frequency rectification into our roadway systems and eliminate batteries in our electric cars and trucks [240]!

Finally, we want to end on a positive note with a very recent result from the NASA JPL microwave limb sounding team. They reported in [71] that the impacts of climate change on atmospheric circulation have shortened the expected lifetime for nitrous oxide to remain in the stratosphere and they predict 27% less N_2O by the end of the 21st century than had been estimated previously. This decrease of N_2O would have a positive effect in slightly reducing global warming and ozone depletion.

With that, we think we have covered about as much of this intersecting technology as we have space for!

VII. SUMMARY

In this broad tutorial we have tried to cover some of the science and applications that bring together the study and observations of climate change, with microwave technology and instrumentation. On the global scale, nothing competes with the ingenious and evolving technological achievements that have filled our skies with complex, multispectral satellite instruments that can make incredibly accurate and sophisticated

observations of physical parameters as diverse as highly accurate temperature profiling from space and backscattering from deep underground snow-ice and water-ice boundaries. Even more impressive is our ever increasingly erudite toolkit for pulling out shrouded or completely hidden physical attributes and resources from observed data when these are coupled with highly developed and vetted mathematical models – using slight changes in the orbital motion of a small object circling the Earth to infer the volume and depth of a buried water reservoir 2000 km below! We truly need to show more respect and homage to our world's scientists and engineers than most of our fellow Earthlings are willing to admit.

As we look closer to home, there are still many impacts of climate change that can be either helped directly, or indirectly, through the application of techniques and instruments that are centered around the microwave spectrum from (as the IEEE Microwave Theory and Technology society likes to advertise) MHz to THz. These take the general form of efficient or specialized heating, chemical conversion for green fuel production and carbon capture, clean power generation through fusion, and perhaps even wireless power transport. Many less impactful cross-connections can be found, and these authors hope the readers of this article will respond with additional collaborative work that brings the microwave engineering community and the climate science community into closer synergy.

ACKNOWLEDGMENT

The authors wish to thank the editorial board and sponsors of the IEEE JOURNAL OF MICROWAVES and the reviewers for allowing this series to get started. They also thank the MIT Libraries' Distinctive Collections for a reprint of the R.S. Bender, A.E. Brent and J.W. Miller Radiation Lab series report in footnote 3.

REFERENCES

[1] G. Breit and M. A. Tuve, "A radio method of estimating the height of the conducting layer," *Nature*, vol. 116, 1925, Art. no. 357.
[2] G. Breit and M. A. Tuve, "A test of the existence of the conducting layer," *Phys. Rev.*, vol. 28, no. 3, pp. 554–575, Sep. 1926.
[3] G. Boudouris, "On the index of refraction of air, the absorption and dispersion of centimeter waves by gases," *J. Res. Nat. Bur. Standards D, Radio Propag.*, vol. 67, no. 6, pp. 631–684, 1963.
[4] F. T. Ulaby, R. K. Moore, and A. K. Fung, *Microwave Remote Sensing: Active and Passive, Volume 1: Fundamentals and Radiometry*. Norwood, MA, USA: Artech House, 1981.
[5] L. N. Ridenour, *Radar System Engineering* (MIT Radiation Laboratory Series), vol. 1. New York, NY, USA: McGraw-Hill, 1947.
[6] F. T. Ulaby, R. K. Moore, and A. K. Fung, *Microwave Remote Sensing: Active and Passive, Volume 2: Radar Remote Sensing and Surface Scattering and Emission Theory*. Norwood, MA, USA: Artech House, 1982.
[7] F. T. Ulaby, R. K. Moore, and A. K. Fung, *Microwave Remote Sensing: Active and Passive, Volume 3: From Theory to Applications*. Norwood, MA, USA: Artech House, 1986.
[8] F. T. Ulaby and D. Long, *Microwave Radar and Radiometric Remote Sensing*. Norwood, MA, USA: Artech House, 2015.
[9] P. H. Siegel, "Microwave pioneers: Charles Elachi, dare mighty things," *IEEE. J. Microwaves*, vol. 2, no. 1, pp. 13–22, Jan. 2022.
[10] C. Elachi and J. V. Zyl, *Introduction to the Physics and Techniques of Remote Sensing*, 3rd ed. Hoboken, NJ, USA: Wiley, 2021.
[11] R. H. Dicke, "The measurement of thermal radiation at microwave frequencies," *Rev. Sci. Instrum.*, vol. 17, no. 7, pp. 268–275, Jul. 1946.
[12] R. H. Dicke, R. Beringer, R. L. Kyhl, and A. B. Vane, "Atmospheric absorption measurements with a microwave radiometer," *Phys. Rev.*, vol. 70, no. 5/6, pp. 340–348, Sep. 1946.
[13] F. Ulaby, "Passive microwave remote sensing of the Earth's surface," *IEEE Trans. Antennas Propag.*, vol. 24, no. 1, pp. 112–115, Jan. 1976.
[14] D. H. Staelin, "Passive remote sensing at microwave wavelengths," *Proc. IEEE*, vol. 57, no. 4, pp. 427–439, Apr. 1969.
[15] J. D. Kraus, *Radio Astronomy*. New York, NY, USA: McGraw-Hill, 1966.
[16] J. W. Waters, "Submillimeter-wavelength heterodyne spectroscopy and remote-sensing of the upper-atmosphere," *Proc. IEEE*, vol. 80, no. 11, pp. 1679–1701, Nov. 1992.
[17] F. T. Barath, A. H. Barrett, J. Copeland, D. E. Jones, and A. E. Lilley, "Mariner II: Preliminary reports on measurements of Venus - microwave radiometers," *Science*, vol. 139, no. 3558, pp. 908–909, Mar. 1963.
[18] F. T. Barath, A. H. Barrett, J. Copeland, D. E. Jones, and A. E. Lilly, "Symposium on radar and radiometric observations of Venus during the 1962 conjunction: Mariner 2 microwave radiometer experiment and results," *Astronomical J.*, vol. 69, no. 1, pp. 49–58, Feb. 1964.
[19] B. G. Kutuza, L. M. Mitnik, and A. B. Akvilonova, "The world's first experiment on microwave Earth sensing from space on the Kosmos-243 satellite," *Curr. Problems Remote Sens. Earth Space*, vol. 16, no. 6, pp. 9–30, 2019.
[20] P. H. Siegel, "THz pioneers: Joe W. Waters: THz meets Gaia," *IEEE Trans. THz Sci. Technol.*, vol. 5, no. 6, pp. 862–883, Nov. 2015.
[21] J. W. Waters et al., "The UARS and EOS microwave limb sounder (MLS) experiments," *J. Atmospheric Sci.*, vol. 56, no. 2, pp. 194–218, Feb. 1999.
[22] D. H. Staelin et al., "Microwave spectrometer on the nimbus 5 satellite: Meteorological and geophysical data," *Science*, vol. 182, no. 4119, pp. 1339–1341, Dec. 1973.
[23] J. W. Waters, K. F. Kunzi, R. L Pettyjohn, R. K. L. Poon, and D. H. Staelin, "Remote sensing of atmospheric temperature profiles with the nimbus 5 microwave spectrometer," *J. Atmospheric Sci.*, vol. 32, no. 10, pp. 1953–1969, 1973.
[24] E. G. Njoku, J. M. Stacey, and F. T. Barath, "The Seasat scanning multichannel microwave radiometer (SMMR): Instrument description and performance," *IEEE J. Ocean. Eng.*, vol. 5, no. 2, pp. 100–115, Apr. 1980, doi: 10.1109/JOE.1980.1145458.
[25] E. G. Njoku, "Passive microwave remote sensing of the Earth from space," *Proc. IEEE*, vol. 70, no. 7, pp. 728–750, Jul. 1982.
[26] I. Galin, D. H. Brest, and G. R. Martner, "The DMSP SSM/T-2 microwave water-vapor profiler," *Proc. SPIE*, vol. 1935, pp. 189–198, 1993.
[27] National Environmental Satellite Data and Information Service, "Joint polar satellite system," 2023. Accessed: Apr. 24, 2023. [Online]. Available: https://www.nesdis.noaa.gov/current-satellite-missions/currently-flying/joint-polar-satellite-system
[28] Wikipedia, "Weather system follow-on microwave," Apr. 11, 2023. Accessed: Apr. 14, 2023. [Online]. Available: https://en.wikipedia.org/wiki/Weather_System_Follow-on_Microwave
[29] NASA's National Snow and Ice Data Center, "MEaSUREs calibrated enhanced-resolution passive microwave daily EASE-Grid 2.0 brightness temperature ESDR, version 1," 2023. Accessed: Apr. 22, 2023. [Online]. Available: https://nsidc.org/data/nsidc-0630/versions/1
[30] Orbital Micro Systems, "Global environmental monitoring system (GEMS)," 2023. Accessed: Apr. 16, 2023. [Online]. Available: https://www.orbitalmicro.com/gems
[31] J. X. Yang et al., "Atmospheric humidity and temperature sounding from the CubeSat TROPICS mission: Early performance evaluation with MiRS," *Remote Sens. Environ.*, vol. 287, 2023, Art. no. 113479.
[32] T. J. Schmugge, P. Gloersen, T. T. Wilheit, and F. Geiger, "Remote sensing of soil moisture with microwave radiometers," *J. Geophys. Res.*, vol. 79, pp. 317–323, 1974.
[33] S. Brönnimann, J. Luterbacher, T. Ewen, H. Diaz, R. Stolarski, and U. Neu, Eds., "Climate variability and extremes during the past 100 years," in *Advances in Global Change Research*, vol. 33. Berlin, Germany: Springer, 2008.
[34] J. W. Waters et al., "Stratospheric ClO and ozone from the microwave limb sounder on the upper atmosphere research satellite," *Nature*, vol. 362, pp. 597–602, 1993.
[35] Q. Zhao et al., "An overview of the applications of earth observation satellite data: Impacts and future trends," *Remote Sens.*, vol. 14, no. 8, Apr. 2022, Art. no. 1863, doi: 10.3390/rs14081863.

[36] D. Ermakov et al., "Comparison of vertically integrated fluxes of atmospheric water vapor according to satellite radiothermovision, radiosondes, and reanalysis," *Remote Sens.*, vol. 13, no. 9, May 2021, Art. no. 1639.
[37] J. Yue et al., "Increasing water vapor in the stratosphere and mesosphere after 2002," *Geophys. Res. Lett.*, vol. 46, no. 22, pp. 13452–13460, Nov. 2019.
[38] N. J. Livesy et al., "Investigation and amelioration of long-term instrumental drifts in water vapor and nitrous oxide measurements from the aura microwave limb sounder (MLS) and their implications for studies of variability and trends," *Atmospheric Chem. Phys.*, vol. 21, no. 20, pp. 15409–15430, Oct. 2021.
[39] E. G. Njoku and L. Li, "Retrieval of land surface parameters using passive microwave measurements at 6-18 GHz," *IEEE Trans. Geosci. Remote Sens.*, vol. 37, no. 1, pp. 79–93, Jan. 1999.
[40] W. Berg et al., "Fundamental climate data records of microwave brightness temperatures," *Remote Sens.*, vol. 10, no. 8, Aug. 2018, Art. no. 1306.
[41] P. Basili, S. Bonafoni, P. Ciotti, F. S. Marzano, G. d'Auria, and N. Pierdicca, "Retrieving atmospheric temperature profiles by microwave radiometry using a priori information on atmospheric spatial-temporal evolution," *IEEE Trans. Geosci. Remote Sens.*, vol. 39, no. 9, pp. 1896–1905, Sep. 2001.
[42] A. E. Lipton, "Polarization of measurement for microwave temperature sounding of the mesosphere," *IEEE Trans. Geosci. Remote Sens.*, vol. 40, no. 8, pp. 1669–1681, Aug. 2002.
[43] Q. H. Liu and F. Weng, "One-dimensional variational retrieval algorithm of temperature, water vapor, and cloud water profiles from advanced microwave sounding unit (AMSU)," *IEEE Trans. Geosci. Remote Sens.*, vol. 43, no. 5, pp. 1087–1095, May 2005.
[44] E. R. Kursinski et al., "The active temperature, ozone and moisture microwave spectrometer (ATOMMS), a new global climate sensor," in *Proc. IEEE Int. Geosci. Remote Sens. Symp.*, 2010, pp. 2952–2955.
[45] J. Du, J. S. Kimball, and L. A. Jones, "Satellite microwave retrieval of total precipitable water vapor and surface air temperature over land from AMSR2," *IEEE Trans. Geosci. Remote Sens.*, vol. 53, no. 5, pp. 2520–2531, May 2015.
[46] W. J. Randel et al., "Stratospheric temperature trends over 1979–2015 derived from combined SSU, MLS, and SABER satellite observations," *J. Climate*, vol. 29, no. 13, pp. 4843–4859, Jul. 2016.
[47] S. J. Munchak, S. Ringerud, L. Brucker, Y. You, I. de Gelis, and C. Prigent, "An active-passive microwave land surface database from GPM," *IEEE Trans. Geosci. Remote Sens.*, vol. 58, no. 9, pp. 6224–6242, Sep. 2020.
[48] E. Defer, C. Jimenez, and C. Prigent, "Sub-millimetre wave radiometry for cloud and rain characterization: From simulation to Earth observation mission concept," *Comptes Rendus Physique*, vol. 13, no. 1, pp. 54–61, Jan./Feb. 2012.
[49] T. Kubota et al., "Global precipitation map using satellite-borne microwave radiometers by the GSMaP project: Production and validation," *IEEE Trans. Geosci. Remote Sens.*, vol. 45, no. 7, pp. 2259–2275, Jul. 2007.
[50] E. Alerskans et al., "Construction of a climate data record of sea surface temperature from passive microwave measurements," *Remote Sens. Environ.*, vol. 236, Jan. 2020, Art. no. 111485.
[51] K. Edokossi et al., "GNSS-reflectometry and remote sensing of soil moisture: A review of measurement techniques, methods, and applications," *Remote Sens.*, vol. 12, no. 4, Feb. 2020, Art. no. 614.
[52] E. Babaeian et al., "Ground, proximal, and satellite remote sensing of soil moisture," *Rev. Geophys.*, vol. 57, no. 2, pp. 530–616, Jun. 2019.
[53] L. Karthikeyan et al., "Four decades of microwave satellite soil moisture observations: Part 1. A review of retrieval algorithms," *Adv. Water Resour.*, vol. 109, pp. 106–120, Nov. 2017.
[54] T. J. Hewison, "Airborne measurements of forest and agricultural land surface emissivity at millimeter wavelengths," *IEEE Trans. Geosci. Remote Sens.*, vol. 39, no. 2, pp. 393–400, Feb. 2001.
[55] S. Paloscia, P. Pampaloni, and E. Santi, "Radiometric microwave indices for remote sensing of land surfaces," *Remote Sens.*, vol. 10, no. 12, Dec. 2018, Art. no. 1859.
[56] B. E. Goodison and A. E. Walker, "Use of snow cover derived from satellite passive microwave data as an indicator of climate-change," *Ann. Glaciol.*, vol. 17, pp. 137–142, 1993.
[57] N. Alimasi, "A review of passive microwave observations of snow-covered areas over complex Arctic terrain," *Bull. Glaciological Res.*, vol. 36, pp. 1–13, 2018.
[58] A. Braakmann-Folgmann and C. Donlon, "Estimating snow depth on Arctic sea ice using satellite microwave radiometry and a neural network," *Cryosphere*, vol. 13, no. 9, pp. 2421–2438, Sep. 2019.
[59] D. Houtz et al., "Snow wetness and density retrieved from L-band satellite radiometer observations over a site in the West Greenland ablation zone," *Remote Sens. Environ.*, vol. 235, Dec. 2019, Art. no. 111361.
[60] N. Reul et al., "Sea surface salinity estimates from spaceborne L-band radiometers: An overview of the first decade of observation (2010–2019)," *Remote Sens. Environ.*, vol. 242, Jun. 2020, Art. no. 111769.
[61] V. V. Tikhonov et al., "Satellite microwave radiometry of sea ice of polar regions: A review," *Izvestiya Atmospheric Ocean. Phys.*, vol. 52, no. 9, pp. 1012–1030, Dec. 2016.
[62] S.-M. Lee, W. N. Meier, B.-J. Sohn, H. Shi, and A. J. Gasiewski, "Estimation of arctic basin-scale sea ice thickness from satellite passive microwave measurements," *IEEE Trans. Geosci. Remote Sens.*, vol. 59, no. 7, pp. 5841–5850, Jul. 2021.
[63] A. C. Bliss et al., "Regional variability of Arctic sea ice seasonal change climate indicators from a passive microwave climate data record," *Environ. Res. Lett.*, vol. 14, no. 4, Apr. 2019, Art. no. 045003.
[64] N. Skou, "Microwave radiometry for oil pollution monitoring, measurements, and systems," *IEEE Trans. Geosci. Remote Sens.*, vol. GE-24, no. 3, pp. 360–367, May 1986.
[65] O. P. N. Calla, H. K. Dadhich, and S. Singhal, "Oil spill detection using multi frequency microwave sensor onboard satellite; SSM/I and AMSR-E," in *Proc. IEEE Int. Geosci. Remote Sens. Symp.*, 2013, pp. 3710–3713.
[66] T. A. Alekseeva et al., "Analysis of sea-ice areas undetectable by the ASI algorithm based on satellite microwave radiometry in the Arctic Ocean," *Izvestiya Atmospheric Ocean. Phys.*, vol. 57, no. 12, pp. 1690–1704, Dec. 2021.
[67] S. T. A. Raj et al., "Long-term trends in stratospheric ozone, temperature, and water vapor over the Indian region," *Annales Geophysicae*, vol. 36, no. 1, pp. 149–165, Jan. 2018.
[68] H. M. Pickett, "THz spectroscopy of the atmosphere," *Proc. SPIE*, vol. 3617, pp. 2–6, 1999.
[69] A. K. Keshari and R. P. Singh, "Assessment of global environment using microwave radiometry," *Glob. Change Space Observ.*, vol. 14, no. 1, pp. 233–236, 1993.
[70] B. M. Quine et al., "The concentration profile of nitric acid and other species over Saskatchewan in August 1998: Retrieval from data recorded by thermal-emission radiometry," *Atmos.-Ocean*, vol. 43, no. 4, pp. 361–376, Dec. 2005.
[71] M. J. Prather, L. Froidevaux, and N. J. Livesey, "Observed changes in stratospheric circulation: Decreasing lifetime of N2O, 2005–2021," *Atmospheric Chem. Phys.*, vol. 23, pp. 843–849, 2023.
[72] C. Prigent, W. B. Rossow, and E. Matthews, "Global maps of microwave land surface emissivities: Potential for land surface characterization," *Radio Sci.*, vol. 33, no. 3, pp. 745–751, May/Jun. 1998.
[73] Y. Kim, J. S. Kimball, K. C. McDonald, and J. Glassy, "Developing a global data record of daily landscape freeze/thaw status using satellite passive microwave remote sensing," *IEEE Trans. Geosci. Remote Sens.*, vol. 49, no. 3, pp. 949–960, Mar. 2011.
[74] F. S. Marzano, A. Mugnai, G. Panegrossi, N. Pierdicca, E. A. Smith, and J. Turk, "Bayesian estimation of precipitating cloud parameters from combined measurements of spaceborne microwave radiometer and radar," *IEEE Trans. Geosci. Remote Sens.*, vol. 37, no. 1, pp. 596–613, Jan. 1999.
[75] T. T. Wilheit and K. D. Hutchison, "Retrieval of cloud base heights from passive microwave and cloud top temperature data," *IEEE Trans. Geosci. Remote Sens.*, vol. 38, no. 3, pp. 1253–1259, May 2000.
[76] B. Bizzarri et al., "Instruments and system for CLOUDS - a cloud and radiation monitoring satellite," *Proc. SPIE*, vol. 4169, pp. 279–290, 2000.
[77] K. F. Evans et al., "The prospect for remote sensing of cirrus clouds with a submillimeter-wave spectrometer," *J. Appl. Meteorol.*, vol. 38, no. 5, pp. 514–525, May 1999.
[78] J. Miao, K.-P. Johnsen, S. Kern, G. Heygster, and K. Kunzi, "Signature of clouds over Antarctic sea ice detected by the special sensor microwave/imager," *IEEE Trans. Geosci. Remote Sens.*, vol. 38, no. 5, pp. 2333–2344, Sep. 2000.
[79] X.-M. Zhu et al., "Estimate of cloudy-sky surface emissivity from passive microwave satellite data using machine learning," *IEEE Trans. Geosci. Remote Sens.*, vol. 60, 2022, Art. no. 4511420.

[80] J. R. Piepmeier and A. J. Gasiewski, "High-resolution passive polarimetric microwave mapping of ocean surface wind vector fields," *IEEE Trans. Geosci. Remote Sens.*, vol. 39, no. 3, pp. 606–622, Mar. 2001.

[81] J. W. Sapp et al., "Stepped frequency microwave radiometer wind-speed retrieval improvements," *Remote Sens.*, vol. 11, no. 3, Feb. 2019, Art. no. 214.

[82] J. F. Galantowicz, "High-resolution flood mapping from low-resolution passive microwave data," in *Proc. IEEE Int. Symp. Geosci. Remote Sens.*, 2002, pp. 1499–1502.

[83] S.-A. Boukabara, F. Weng, and Q. Liu, "Passive microwave remote sensing of extreme weather events using NOAA-18 AMSUA and MHS," *IEEE Trans. Geosci. Remote Sens.*, vol. 45, no. 7, pp. 2228–2246, Jul. 2007.

[84] E. J. Zipser et al., "Where are the most intense thunderstorms on Earth?," *Bull. Amer. Meteorological Soc.*, vol. 87, no. 8, Aug. 2006, Art. no. 1057.

[85] B. Zhang, Z. Q. Zhu, W. Perrie, J. Tang, and J. A. Zhang, "Estimating tropical cyclone wind structure and intensity from spaceborne radiometer and synthetic aperture radar," *IEEE J. Sel. Topics Appl. Earth Observ. Remote Sens.*, vol. 14, pp. 4043–4050, 2021.

[86] G. S. Zhang, C. Xu, X. Li, Z. Zhu, and W. Perrie, "Tropical Cyclone center and symmetric structure estimating from SMAP data," *IEEE Trans. Geosci. Remote Sens.*, vol. 60, 2022, Art. no. 4205311.

[87] T. Meissner and F. J. Wentz, "Wind-vector retrievals under rain with passive satellite microwave," *IEEE Trans. Geosci. Remote Sens.*, vol. 47, no. 9, pp. 3065–3083, Sep. 2009.

[88] M. Montopoli, D. Cimini, M. Lamantea, M. Herzog, H. F. Graf, and F. S. Marzano, "Microwave radiometric remote sensing of volcanic ash clouds from space: Model and data analysis," *IEEE Trans. Geosci. Remote Sens.*, vol. 51, no. 9, pp. 4678–4691, Sep. 2013.

[89] F. S. Marzano et al., "Microwave remote sensing of the 2011 Plinian Eruption of the Grimsvotn Icelandic volcano," *Remote Sens. Environ.*, vol. 129, pp. 168–184, Feb. 2013.

[90] F. Romeo et al., "Volcanic cloud detection and retrieval using satellite multisensor observations," *Remote Sens.*, vol. 15, no. 4, p. 888, Feb. 2023.

[91] J. H. van Vleck, "The absorption of microwaves by uncondensed water vaper," *Phys. Rev.*, vol. 71, no. 7, pp. 425–433, Apr. 1947.

[92] R. S. Bender, A. E. Brent, and J. W. Miller, "An aerial investigation of K-band radar performance under tropical atmospheric conditions," MIT Radiation Laboratory report 179, pp. 1–45, Oct. 1, 1945.

[93] A. F. Spilhaus, "Drop size, intensity, and radar echo of rain," *J. Atmospheric Sci.*, vol. 5, no. 4, pp. 161–164, 1948.

[94] L. J. Cutrona and G. O. Hall, "A comparison of techniques for achieving fine azimuth resolution," *Inst. Radio Engineers Trans. Mil. Electron.*, vol. MIL-6, no. 2, pp. 119–121, Apr. 1962.

[95] C. W. Sherwin, J. P. Ruina, and R. D. Rawcliffe, "Some early developments in synthetic aperture radar systems," *Inst. Radio Engineers Trans. Mil. Electron.*, vol. MIL-6, no. 2, pp. 111–115, Apr. 1962.

[96] J. A. Develet, "Performance of a synthetic-aperture mapping radar system," *IEEE Trans. Aerosp. Navigational Electron.*, vol. ANE-11, no. 3, pp. 173–179, Sep. 1964.

[97] C. D. Leitao and J. T. McGoogan, "Skylab radar altimeter: Short-wavelength perturbations detected in ocean surface profiles," *Science*, vol. 186, no. 4170, pp. 1208–1209, Dec. 1974.

[98] R. K. Moore and F. T. Ulaby, "The radar radiometer," *Proc. IEEE*, vol. 57, no. 4, pp. 587–590, Apr. 1969.

[99] C. Elachi, "Wave patterns across North-Atlantic on September 28, 1974, From airborne radar imagery," *J. Geophys. Res., Oceans Atmospheres*, vol. 81, no. 15, pp. 2655–2656, 1976.

[100] R. L. Jordan, "The Seasat-a synthetic aperture radar system," *IEEE J. Ocean. Eng.*, vol. OE-5, no. 2, pp. 154–164, Apr. 1980.

[101] R. G. Blom, R. E. Crippen, and C. Elachi, "Detection of subsurface features in Seasat radar images of means valley, Mojave-desert, California," *Geology*, vol. 12, no. 6, pp. 346–349, 1984.

[102] C. Elachi, "Spaceborne imaging radar - geologic and oceanographic applications," *Science*, vol. 209, no. 4461, pp. 1073–1082, 1980.

[103] D. L. Evans et al., "Seasat - a 25-year legacy of success," *Remote Sens. Environ.*, vol. 94, no. 3, pp. 384–404, Feb. 2005.

[104] D. Atlas, C. Elachi, and W. E. Brown, "Precipitation mapping with an airborne synthetic aperture imaging radar," *J. Geophys. Res., Oceans Atmospheres*, vol. 82, no. 24, pp. 3445–3451, 1977.

[105] C. Elachi, "Earth resources observation with the shuttle imaging radar," *Proc. SPIE*, vol. 278, pp. 73–78, 1981.

[106] C. Elachi, K. E. Im, F. Li, and E. Rodriguez, "Global digital topography mapping with a synthetic aperture scanning radar altimeter," *Int. J. Remote Sens.*, vol. 11, no. 4, pp. 585–601, Apr. 1990.

[107] N. Y. Wang and P. S. Chang, "WindSat physically-based forward model: Atmospheric component," *Proc. SPIE*, vol. 5656, pp. 104–110, 2005.

[108] E. N. Anagnostou, "Overview of overland satellite rainfall estimation for hydro-meteorological applications," *Surv. Geophys.*, vol. 25, no. 5/6, pp. 511–537, Nov. 2004.

[109] B. Bizzarri et al., "Instruments and system for CLOUDS - a cloud and radiation monitoring satellite," *Proc. SPIE*, vol. 4169, pp. 279–290, 2000.

[110] Y. W. Chen et al., "UAV-borne profiling radar for forest research," *Remote Sens.*, vol. 9, no. 1, Jan. 2017, Art. no. 58.

[111] F. Frappart et al., "Global monitoring of the vegetation dynamics from the vegetation optical depth (VOD): A review," *Remote Sens.*, vol. 12, no. 18, Sep. 2020, Art. no. 2915.

[112] M. Shimada and A. Rosenqvist, "Advanced land observing satellite (ALOS) and monitoring global environmental change," *Proc. IEEE*, vol. 98, no. 5, pp. 780–799, May 2021.

[113] Y. Aimaiti, A. Kasimu, and G. Jing, "Urban landscape extraction and analysis based on optical and microwave ALOS satellite data," *Earth Sci. Inform.*, vol. 9, no. 4, pp. 425–435, Nov. 2016.

[114] L. Karthikeyan, I. Chawla, and A. K. Mishra, "A review of remote sensing applications in agriculture for food security: Crop growth and yield, irrigation, and crop losses," *J. Hydrol.*, vol. 586, Jul. 2020, Art. no. 124905.

[115] K. Y. Guan et al., "The shared and unique values of optical, fluorescence, thermal and microwave satellite data for estimating large-scale crop yields," *Remote Sens. Environ.*, vol. 199, pp. 333–349, Sep. 2017.

[116] M. K. Mosleh, Q. K. Hassan, and E. H. Chowdhury, "Application of remote sensors in mapping rice area and forecasting its production: A review," *Sensors*, vol. 15, no. 1, pp. 769–791, Jan. 2015.

[117] R. K. Zhao, Y. C. Li, and M. G. Ma, "Mapping paddy rice with satellite remote sensing: A review," *Sustainability*, vol. 13, no. 2, Jan. 2021, Art. no. 503.

[118] W. Koppe et al., "Multi-temporal hyperspectral and radar remote sensing for estimating winter wheat biomass in the North China plain," *Photogrammetrie Fernerkundung Geoinformation*, vol. 3, pp. 281–298, 2012.

[119] T. Lopez, A. Al Bitar, S. Biancamaria, A. Guntner, and A. Jaggi, "On the use of satellite remote sensing to detect floods and droughts at large scales," *Surv. Geophys.*, vol. 41, no. 6, pp. 1461–1487, Nov. 2020.

[120] T. Manninen, P. Stenberg, M. Rautiainen, and P. Voipio, "Leaf area index estimation of boreal and subarctic forests using VV/HH ENVISAT/ASAR data of various swaths," *IEEE Trans. Geosci. Remote Sens.*, vol. 51, no. 7, pp. 3899–3909, Jul. 2013.

[121] R. K. Ningthoujam et al., "Mapping forest cover and forest cover change with airborne S-band radar," *Remote Sens.*, vol. 8, no. 7, Jul. 2016, Art. no. 577.

[122] J. Seppanen, O. Antropov, T. Jagdhuber, M. Hallikainen, J. Heiskanen, and J. Praks, "Improved characterization of forest transmissivity within the L-MEB model using multisensor SAR data," *IEEE Geosci. Remote Sens. Lett.*, vol. 14, no. 8, pp. 1408–1412, Aug. 2017.

[123] J. Widodo et al., "Forest areas with a high potential risk of fire mapping on peatlands using interferometric synthetic aperture radar," in *Proc. IEEE 7th Asia-Pacific Conf. Synthetic Aperture Radar*, 2021, pp. 1–4.

[124] L. L. Bourgeau-Chavez, E. S. Kasischke, and M. D. Rutherford, "Evaluation of ERS SAR data for prediction of fire danger in a boreal region," *Int. J. Wildland Fire*, vol. 9, no. 3, pp. 183–194, Dec. 1999.

[125] M. A. Rahman et al., "Weather radar detection of planetary boundary layer and smoke layer top of peatland fire in Central Kalimantan, Indonesia," *Sci. Rep.*, vol. 11, no. 1, pp. 1–9, Jan. 2021.

[126] J. Murfitt and C. R. Duguay, "50 years of lake ice research from active microwave remote sensing: Progress and prospects," *Remote Sens. Environ.*, vol. 264, Oct. 2021, Art. no. 112616.

[127] R. Bindschadler, "Monitoring ice sheet behavior from space," *Rev. Geophys.*, vol. 36, no. 1, pp. 79–104, Feb. 1998.

[128] M. G. Cooper and L. C. Smith, "Satellite remote sensing of the Greenland ice sheet ablation zone: A review," *Remote Sens.*, vol. 11, no. 20, Oct. 2019, Art. no. 2405.

[129] J. M. Piwowar and E. F. Ledrew, "Hypertemporal analysis of remotely-sensed sea-ice data for climate-change studies," *Prog. Phys. Geography*, vol. 19, no. 2, pp. 216–242, Jun. 1995.

[130] K. Lane, D. Power, J. Youden, C. Randell, and D. Flett, "Validation of synthetic aperture radar for iceberg a detection in sea ice," in *Proc. IEEE Int. Geosci. Remote Sens. Symp.*, 2004, pp. 125–128.
[131] M. K. Singh Snehmani, R. D. Gupta, A. Bhardwaj, and P. K. Joshi, "Remote sensing of mountain snow using active microwave sensors: A review," *Geocarto Int.*, vol. 30, no. 1, pp. 1–27, Jan. 2015.
[132] L. Tsang et al., "Review article: Global monitoring of snow water equivalent using high-frequency radar remote sensing," *Cryosphere*, vol. 16, no. 9, pp. 3531–3573, Sep. 2022.
[133] H. Jafarzadeh, M. Mahdianpari, S. Homayouni, F. Mohammadimanesh, and M. Dabboor, "Oil spill detection from synthetic aperture radar earth observations: A meta-analysis and comprehensive review," *Giscience Remote Sens.*, vol. 58, no. 7, pp. 1022–1051, Oct. 2021.
[134] M. Fingas and C. E. Brown, "A review of oil spill remote sensing," *Sensors*, vol. 18, no. 1, Jan. 2018, Art. no. 91.
[135] E. Babaeian, M. Sadeghi, S. B. Jones, C. Montzka, H. Vereecken, and M. Tuller, "Ground, proximal, and satellite remote sensing of soil moisture," *Rev. Geophys.*, vol. 57, no. 2, pp. 530–616, Jun. 2019.
[136] R. van der Schalie et al., "L-band soil moisture retrievals using microwave based temperature and filtering. towards model-independent climate data records," *Remote Sens.*, vol. 13, no. 13, Jul. 2021, Art. no. 2480.
[137] J. Peng et al., "A roadmap for high-resolution satellite soil moisture applications - confronting product characteristics with user requirements," *Remote Sens. Environ.*, vol. 252, Jan. 2021, Art. no. 112162.
[138] T. J. Zhao et al., "Retrievals of soil moisture and vegetation optical depth using a multi-channel collaborative algorithm," *Remote Sens. Environ.*, vol. 257, May 2021, Art. no. 112321.
[139] A. Kaab et al., "Remote sensing of glacier- and permafrost-related hazards in high mountains: An overview," *Natural Hazards Earth Syst. Sci.*, vol. 5, no. 4, pp. 527–554, 2005.
[140] J. Wang, H. G. Zhang, J. S. Yang, L. Ren, and X. Z. Wang, "A new mapping method of underwater bottom topography in the shallow sea by using SAR images," *Proc. SPIE*, vol. 9999, pp. 26–27, 2016.
[141] B. D. Tapley et al., "Contributions of GRACE to understanding climate change," *Nature Climate*, vol. 9, no. 5, pp. 358–369, May 2019.
[142] K. B. Cooper et al., "G-band radar for humidity and cloud remote sensing," *IEEE Trans. Geosci. Remote Sens.*, vol. 59, no. 2, pp. 1106–1117, Feb. 2021.
[143] M. Schandri, M. Zink, and M. Bachmann, "TanDEM-X mission status and outlook on the tandem-L mission," in *Proc. IEEE 23rd Int. Radar Symp.*, 2022, pp. 443–446.
[144] NASA, "NASA airborne science program, platforms," Apr. 22, 2017. Accessed: Apr. 22, 2023. [Online]. Available: https://airbornescience.nasa.gov/platform/comparison
[145] NASA, "NASA airborne science program, missions," Apr. 22, 2017. Accessed: Apr. 22, 2023. [Online]. Available: https://airbornescience.nasa.gov/program/airborne_missions
[146] D. A. Deisinger, "Development of meteorological instrumentation at USASRDL," *Int. Rev. Educ. Trans. Mil. Electron.*, vol. MIL-4, no. 4, pp. 572–583, Oct. 1960.
[147] V. E. Noble, R. D. Ketchum, and D. B. Ross, "Some aspects of remote sensing as applied to oceanography," *Proc. IEEE*, vol. 57, no. 4, pp. 594–604, Apr. 1969.
[148] W. E. Brown and C. Elachi, "Imaging radar potentials for Earth resources," in *Proc. IEEE Microw. Theory Technol. Soc. Int. Microw. Symp.*, 1975, pp. 29–31.
[149] F. T. Ulaby, W. H. Stiles, L. F. Dellwig, and B. C. Hanson, "Experiments on the radar backscatter of snow," *IEEE Trans. Geosci. Electron.*, vol. 15, no. 4, pp. 185–189, Oct. 1977.
[150] R. Moore, "Active microwave sensing of the Earth's surface–A mini review," *IEEE Trans. Antennas Propag.*, vol. 26, no. 6, pp. 843–849, Nov. 1978.
[151] M. C. Dobson and F. Ulaby, "Microwave backscatter dependence on surface roughness, soil moisture, and soil texture: Part III-soil tension," *IEEE Trans. Geosci. Remote Sens.*, vol. GE-19, no. 1, pp. 51–61, Jan. 1981.
[152] Y. Furuhama and T. Ihara, "Remote sensing of path-averaged raindrop size distributions from microwave scattering measurements," *IEEE Trans. Antennas Propag.*, vol. TAP-29, no. 2, pp. 275–281, Mar. 1981.
[153] W.-M. Boerner and Y. Yamaguchi, "A state-of-the-art review in radar polarimetry and its applications in remote sensing," *IEEE Aerosp. Electron. Syst. Mag.*, vol. 5, no. 6, pp. 3–6, Jun. 1990.
[154] S. F. Clifford, J. C. Kaimal, R. J. Lataitis, and R. G. Strauch, "Ground-based remote profiling in atmospheric studies: An overview," *Proc. IEEE*, vol. 82, no. 3, pp. 313–355, Mar. 1994.
[155] J. Evans and D. Turnbull, "Development of an automated windshear detection system using doppler weather radar," *Proc. IEEE*, vol. 77, no. 11, pp. 1661–1673, Nov. 1989.
[156] R. Bamler and P. Hartl, "Synthetic aperture radar interferometry," *Inverse Problems*, vol. 14, no. 4, pp. R1–R54, 1998.
[157] A. K. Awasthi et al., "High-sensitivity transceiver for airborne ultra-wideband radio echo sounding of polar regions," in *Proc. IEEE Microw., Antennas, Propag. Conf.*, 2022, pp. 1827–1832.
[158] R. J. Dengler et al., "600 GHz imaging radar with 2 cm range resolution," in *Proc. IEEE Microw. Theory Technol. Soc. Int. Microw. Symp.*, 2007, pp. 1371–1374.
[159] K. B. Cooper et al., "Measuring the 557 GHz Water vapor absorption line with radar speckle averaging," in *Proc. IEEE Microw. Theory Technol. Soc. Int. Microw. Symp.*, 2022, pp. 553–555.
[160] R. Nebuloni, C. Capsoni, and V. Vigorita, "Quantifying bird migration by a high-resolution weather radar," *IEEE Trans. Geosci. Remote Sens.*, vol. 46, no. 6, pp. 1867–1875, Jun. 2008.
[161] J. Liu et al., "Underground coal fires identification and monitoring using time-series InSAR with persistent and distributed scatterers: A case study of Miquan coal fire zone in Xinjiang, China," *IEEE Access*, vol. 7, pp. 164492–164506, 2019.
[162] R. A. Martins, J. M. Felicio, S. A. Matos, J. R. Costa, and C. A. Fernandes, "Preliminary characterization of microwave backscattering of floating plastic," in *Proc. Telecoms Conf.*, 2021, pp. 1–4.
[163] D. Hogg, "Ground-based remote sensing and profiling of the lower atmosphere using radio wavelengths," *IEEE Trans. Antennas Propag.*, vol. 28, no. 2, pp. 281–283, Mar. 1980.
[164] F. T. Ulaby, M. Razani, and M. C. Dobson, "Effects of vegetation cover on the microwave radiometric sensitivity to soil moisture," *IEEE Trans. Geosci. Remote Sens.*, vol. GE-21, no. 1, pp. 51–61, Jan. 1983.
[165] D. R. Brunfeldt and F. T. Ulaby, "Measured microwave emission and scattering in vegetation canopies," *IEEE Trans. Geosci. Remote Sens.*, vol. GE-22, no. 6, pp. 520–524, Nov. 1984.
[166] W. J. Blackwell et al., "NPOESS aircraft sounder Testbed-microwave (NAST-M): Instrument description and initial flight results," *IEEE Trans. Geosci. Remote Sens.*, vol. 39, no. 11, pp. 2444–2453, Nov. 2001.
[167] W. J. Blackwell, F. W. Chen, R. V. Leslie, P. W. Rosenkranz, M. J. Schwartz, and D. H. Staelin, "NPOESS aircraft sounder Testbed-microwave (NAST-M): Results from CAMEX-3 and WINTEX," in *Proc. IEEE Int. Geosci. Remote Sens. Symp. Taking Pulse Planet: Role Remote Sens. Manag. Environ.*, 2000, vol. 2, pp. 803–805.
[168] J. W. Waters, J. C. Hardy, R. F. Jarnot, and H. M. Pickett, "Chlorine monoxide radical, ozone, and hydrogen-peroxide - stratospheric measurements by microwave limb sounding," *Science*, vol. 214, no. 4516, pp. 61–64, 1981.
[169] M. C. Gaidis, H. M. Pickett, C. D. Smith, S. C. Martin, R. P. Smith, and P. H. Siegel, "A 2.5-THz receiver front end for spaceborne applications," *IEEE Trans. Microw. Theory Techn.*, vol. 48, no. 4, pp. 733–739, Apr. 2000.
[170] J. W. Waters, R. A. Stachnik, J. C. Hardy, and R. F. Jarnot, "ClO and O3 stratospheric profiles–balloon microwave measurements," *Geophys. Res. Lett.*, vol. 15, no. 8, pp. 780–783, 1988.
[171] W. J. Wilson and A. B. Taner, "Synthetic aperture imaging radiometer," *Proc. Soc. Photo-Opt. Instrum. Engineers, Microw. Instrum. Remote Sens. Earth*, vol. 1935, pp. 257–262, 1993.
[172] W. J. Wilson, R. J. Howard, A. Ibbott, G. S. Parks, and W. B. Ricketts, "Millimeter-wave imaging sensor," *IEEE Trans. Microw. Theory Techn.*, vol. 34, no. 10, pp. 1026–1035, Oct. 1986.
[173] W. J. Wilson and S. H. Yueh, "JPL wind radiometer measurements," in *Proc. Int. Geosci. Remote Sens. Symp.*, 1996, pp. 1447–1449.
[174] D. K. Hall et al., "Passive microwave remote and in situ measurements of artic and subarctic snow covers in Alaska," *Remote Sens. Environ.*, vol. 38, no. 3, pp. 161–172, Dec. 1991.
[175] T. J. Hewison and S. J. English, "Airborne retrievals of snow and ice surface emissivity at millimeter wavelengths," *IEEE Trans. Geosci. Remote Sens.*, vol. 37, no. 4, pp. 1871–1879, Jul. 1999.
[176] S. Kotthaus et al., "Atmospheric boundary layer height from ground-based remote sensing: A review of capabilities and limitations," *Atmospheric Meas. Tech.*, vol. 16, no. 2, pp. 433–479, Jan. 2023.
[177] B. Shrestha et al., "Overview and applications of the New York State Mesonet profiler network," *J. Appl. Meteorol. Climatol.*, vol. 60, no. 11, pp. 1591–1611, 2021.

[178] L. Zhu et al., "A method for retrieving thermodynamic atmospheric profiles using microwave radiometers of meteorological observation networks," *IEEE Trans. Geosci. Remote Sens.*, vol. 60, 2022, Art. no. 4110311.

[179] D. M. Karavaev et al., "Prospects for application of ground-based microwave radiometry for analysis of atmospheric fronts and early prediction of severe weather events," *Russian Meteorol. Hydrol.*, vol. 47, pp. 946–952, 2022.

[180] H. Gernsback, Ed., "Cooking with shortwaves," in *Short Wave Craft*. Richmond Hill, ON, Canada: Popular Book Corp., 1933, pp. 394–429.

[181] A. W. Hull, "The magnetron," *J. Amer. Inst. Elect. Eng.*, vol. 40, no. 9, pp. 715–723, Sep. 1921.

[182] G. R. Kilgore, "Magnetron oscillators for generation of frequencies between 300 and 600 megacycles," *Proc. Int. Rev. Educ.*, vol. 24, no. 8, pp. 1140–1157, Aug. 1936.

[183] H. A. H Boot and J. T. Randall, "The cavity magnetron," *J. Inst. Electric Eng.*, vol. 93, no. 5, pp. 928–938, 1946.

[184] D. Murray, "Percy spencer and his itch to know," *Reader's Dig.*, vol. 74, no. 436, pp. 114–118, Aug. 1958.

[185] J. M. Osepchuk, "A history of microwave heating applications," *IEEE Trans. Microw. Theory Techn.*, vol. 32, no. 9, pp. 1200–1224, Sep. 1984.

[186] P. H. Siegel, "Microwaves are everywhere: 'Ovens: From magnetrons to metamaterials'," *IEEE J. Microwaves*, vol. 1, no. 2, pp. 523–531, Apr. 2021.

[187] J. C. Atuonwu and S. A. Tassou, "Energy issues in microwave food processing: A review of developments and the enabling potentials of solid-state power delivery," *Crit. Rev. Food Sci. Nutr.*, vol. 59, no. 9, pp. 1392–1407, May 2019.

[188] J. R. G. Twisleton, "Twenty-kilowatt 890 Mc/s continuous-wave magnetron," *Proc. Inst. Elect. Engineers*, vol. 3, no. 1, pp. 51–56, Jan. 1964.

[189] L. Agusu et al., "Detailed design of a 1 THz CW gyrotron (gyrotron FU CW III) using a 20 T superconducting magnet," in *Proc. Int. Kharkov Symp. Phys. Eng. Millimeter Sub-Millimeter Waves*, 2007, pp. 186–188.

[190] M. L. Kulygin, I. A. Litovsky, A. V. Chirkov, I. N. Shevelev, G. I. Kalynova, and M. Y. Shmelev, "Terahertz active nanosecond gigawatt compressor thermal feasibility," in *Proc. IEEE Int. Conf. Microw., Antennas, Commun. Electron. Syst.*, 2021, pp. 99–102.

[191] C. Acar, I. Dincer, and A. Mujumdar, "A comprehensive review of recent advances in renewable-based drying technologies for a sustainable future," *Drying Technol.*, vol. 40, no. 6, pp. 1029–1050, 2022.

[192] D. Wray and H. S. Ramaswamy, "Novel concepts in microwave drying of foods," *Drying Technol.*, vol. 33, pp. 769–783, 2015.

[193] T. Y. A. Fahmy et al., "Biomass pyrolysis: Past, present, and future," *Environ., Develop. Sustainability*, vol. 22, pp. 17–32, 2020, doi: 10.1007/s10668-018-0200-5.

[194] J. P. Kesselring and R. D. Smith, "Development of a microwave clothes dryer," *IEEE Trans. Ind. Appl.*, vol. 32, no. 1, pp. 47–50, Jan./Feb. 1996, doi: 10.1109/28.485811.

[195] A. K. Babu, G. Kumaresan, V. A. A. Raj, and R. Velraj, "Review of leaf drying: Mechanism and influencing parameters, drying methods, nutrient preservation, and mathematical models," *Renewable Sustain. Energy Rev.*, vol. 90, pp. 536–556, Jul. 2018.

[196] M. S. M. Basri et al., "Progress in the valorization of fruit and vegetable wastes: Active packaging, biocomposites, by-products, and innovative technologies used for bioactive compound extraction," *Polymers*, vol. 13, no. 20, Oct. 2021, Art. no. 3503.

[197] P. H. Camani, B. F. Anholon, R. R. Toder, and D. S. Rosa, "Microwave-assisted pretreatment of eucalyptus waste to obtain cellulose fibers," *Cellulose*, vol. 27, no. 7, pp. 3591–3609, May 2020.

[198] X. Feng et al., "Dry heating, moist heating, and microwave irradiation of cold-climate-adapted barley grain—Effects on ruminant-relevant carbohydrate and molecular structural spectral profiles," *J. Animal Physiol. Animal Nutr.*, vol. 107, pp. 113–120, 2023.

[199] H. Ashraf, T. Anjum, S. Riaz, T. Batool, S. Naseem, and G. H. Li, "Sustainable synthesis of microwave-assisted IONPs using Spinacia oleracea L. for control of fungal wilt by modulating the defense system in tomato plants," *J. Nanobiotechnol.*, vol. 20, no. 1, Jan. 2022, Art. no. 8.

[200] G. D. Jimenez et al., "New insights into microwave pyrolysis of biomass: Preparation of carbon-based products from pecan nutshells and their application in wastewater treatment," *J. Anal. Appl. Pyrolysis*, vol. 124, pp. 113–121, 2017.

[201] M. C. Robinson, J. A. Molles, V. V. Yakovlev, and Z. Popović, "Solid-state power combining for heating small volumes of mixed waste materials," *IEEE J. Microwaves*, vol. 3, no. 3, pp. 884–897, 2023, doi: 10.1109/JMW.2023.3259990.

[202] Q. Hou et al., "Biorefinery roadmap based on catalytic production and upgrading 5-hydroxymethylfurfural," *Green Chem., Roy. Soc. Chem.*, vol. 23, pp. 119–231, 2021, doi: 10.1039/d0gc02770g.

[203] United Nations Dept. of Economic and Social Affairs, "Energy Statistics Pocketbook 2022," United Nations, Mar. 2022.

[204] United Nations, "World Food and Agriculture - Statistical Yearbook 2021," FAO report, Rome, Italy, 2021. [Online]. Available: https://doi.org/10.4060/cb4477en.

[205] J.-C. Chen and J.-S. Guo, "Improving the conversion efficiency of waste cotton to bioethanol by microwave hydrolysis technology," *Sustain. Environ. Res.*, vol. 23, no. 5, pp. 333–339, 2013.

[206] S. Aravind, P. S. Kumar, N. S. Kumar, and N. Siddarth, "Conversion of green algal biomass into bioenergy by pyrolysis. A review," *Environ. Chem. Lett.*, vol. 18, no. 3, pp. 829–849, May 2020.

[207] F. Alajmi, A. A. Hairuddin, N. M. Adam, and L. C. Abdullah, "Recent trends in biodiesel production from commonly used animal fats," *Int. J. Energy Res.*, vol. 42, no. 3, pp. 885–902, Mar. 2018.

[208] S. Panigrahi and B. K. Dubey, "A critical review on operating parameters and strategies to improve the biogas yield from anaerobic digestion of organic fraction of municipal solid waste," *Renewable Energy*, vol. 143, pp. 779–797, 2019.

[209] P. Gallezot, "Conversion of biomass into selected chemical products," *Chem. Soc. Rev.*, vol. 41, no. 4, pp. 1538–1558, 2012.

[210] W. Den, V. K. Sharma, M. Lee, G. Nadadur, and R. S. Varma, "Lignocellulosic biomass transformations via greener oxidative pretreatment processes: Access to energy and value-added chemicals," *Front. Chem.*, vol. 6, Apr. 2018, Art. no. 141, doi: 10.3389/fchem.2018.00141.

[211] N. M. Clauser et al., "Biomass waste as sustainable raw material for energy and fuels," *Sustainability*, vol. 13, no. 2, Jan. 2021, Art. no. 794, doi: 10.3390/su13020794.

[212] A. Suresh et al., "Microwave pyrolysis of coal, biomass and plastic waste: A review," *Environ. Chem. Lett.*, vol. 19, no. 5, pp. 3609–3629, Oct. 2021.

[213] V. Hadiya et al., "Biochar production with amelioration of microwave-assisted pyrolysis: Current scenario, drawbacks and perspectives," *Bioresource Technol.*, vol. 355, Jul. 2022, Art. no. 127303, doi: 10.1016/j.biortech.2022.127303.

[214] A. I. Osman et al., "Biochar for agronomy, animal farming, anaerobic digestion, composting, water treatment, soil remediation, construction, energy storage, and carbon sequestration: A review," *Environ. Chem. Lett.*, vol. 20, pp. 2385–2485, 2022.

[215] D. Akhil et al., "Production, characterization, activation and environmental applications of engineered biochar: A review," *Environ. Chem. Lett.*, vol. 19, pp. 2261–2297, 2021, doi: 10.1007/s10311-020-01167-7.

[216] A. George et al., "A review of non-thermal plasma technology: A novel solution for CO_2 conversion and utilization," *Renewable Sustain. Energy Rev.*, vol. 135, 2021, Art. no. 109702, doi: 10.1016/j.rser.2020.109702.

[217] M. Y. Ong, S. Nomanbhay, F. Kusumo, and P. L. Show, "Application of microwave plasma technology to convert carbon dioxide (CO2) into high value products: A review," *J. Cleaner Prod.*, vol. 336, Feb. 2022, Art. no. 130447, doi: 10.1016/j.jclepro.2022.130447.

[218] S. J. McGurk, C. F. Martin, S. Brandani, M. B. Sweatman, and X. F. Fan, "Microwave swing regeneration of aqueous monoethanolamine for post-combustion CO_2 capture," *Appl. Energy*, vol. 192, pp. 126–133, Apr. 2017.

[219] Y. N. Chun and H. G Song, "Microwave induced carbon-CO_2 gasification for energy conversion," *Energy*, vol. 90, 2020, Art. no. 116386.

[220] M. Ambrosetti, "A perspective on power-to-heat in catalytic processes for decarbonization," *Chem. Eng. Process Intensification*, vol. 182, 2022, Art. no. 109187.

[221] J. A. Phillips, "Magnetic fusion," *Los Alamos Sci.*, pp. 64–67, 1983. Accessed: May 8, 2023. [Online]. Available: http://permalink.lanl.gov/object/tr?what=info%3Alanl-repo%2Flareport%2FLA-UR-83-5080.

[222] K. Samanta, "High-power circuits and systems (kWs to MWs) covering MHz to 100s of GHz for nuclear fusion reactors," *IEEE J. Microwaves*, to be published, 2023.

[223] J. R. Pierce and L. M. Field, "Traveling-wave tubes," *Proc. Int. Rev. Educ.*, vol. 35, no. 2, pp. 108–111, Feb. 1947, doi: 10.1109/JRPROC.1947.226216.
[224] A. Beunas et al., "High-power CW klystron for fusion experiments," *IEEE Trans. Electron Devices*, vol. 56, no. 5, pp. 864–869, May 2009, doi: 10.1109/TED.2009.2015807.
[225] M. Thumm, "Recent advances in the worldwide fusion gyrotron development," *IEEE Trans. Plasma Sci.*, vol. 42, no. 3, pp. 590–599, Mar. 2014, doi: 10.1109/TPS.2013.2284026.
[226] W. C. Brown, "The technology and application of free-space power transmission by microwave beam," *Proc. IEEE*, vol. 62, no. 1, pp. 11–25, Jan. 1974.
[227] W. C. Brown and E. E. Eves, "Beamed microwave power transmission and its application to space," *IEEE Trans. Microw. Theory Techn.*, vol. 40, no. 6, pp. 1239–1250, Jun. 1992, doi: 10.1109/22.141357.
[228] C. T. Rodenbeck et al., "Microwave and millimeter wave power beaming," *IEEE J. Microwaves*, vol. 1, no. 1, pp. 229–259, Jan. 2021.
[229] C. T. Rodenbeck et al., "Terrestrial microwave power beaming," *IEEE J. Microwaves*, vol. 2, no. 1, pp. 28–43, Jan. 2022.
[230] N. Shinohara, "History and innovation of wireless power transfer via microwaves," *IEEE J. Microwaves*, vol. 1, no. 1, pp. 218–228, Jan. 2021.
[231] I. Commission on Non-Ionizing Radiation Protection (ICNIRP), "Guidelines for limiting exposure to electromagnetic fields (100 kHz to 300 GHz)," *Health Phys.*, vol. 118, no. 5, pp. 483–524, May 2020.
[232] P. E. Glaser, "Power from the Sun: Its future," *Science*, vol. 162, pp. 957–961, 1968.
[233] G. A. Landis, "RE-evaluating satellite solar power systems for Earth," in *Proc. IEEE 4th World Conf. Photovoltaic Energy Conf.*, 2006, pp. 1939–1942, doi: 10.1109/WCPEC.2006.279877.
[234] News, "In a first, caltech's space solar power demonstrator wirelessly transmits power in space," *The Caltech Weekly*, Jun. 2023. Accessed: Jun. 3, 2023. [Online]. Available: https://www.caltech.edu/about/news/in-a-first-caltechs-space-solar-power-demonstrator-wirelessly-transmits-power-in-space
[235] K. S. Paulson, "The effects of climate change on microwave telecommunications," in *Proc. IEEE 11th Int. Conf. Telecommun.*, 2011, pp. 157–160.
[236] P. Kántor and J. Bitó, "Influence of climate variability on performance of wireless microwave links," in *Proc. IEEE 24th Annu. Int. Symp. Pers., Indoor, Mobile Radio Commun.*, 2013, pp. 891–895, doi: 10.1109/PIMRC.2013.6666263.
[237] G. B. Gratton, P. D. Williams, A. Padhra, and S. Rapsomanikis, "Reviewing the impacts of climate change on air transport operations," *Aeronautical J.*, vol. 126, pp. 209–221, 2022.
[238] J. E. Evans, "Applications of microwave radar to improving aviation safety and efficiency," in *Proc. IEEE Microw. Theory Technol. Soc. Int. Microw. Symp.*, 1998, p. 1935, doi: 10.1109/MWSYM.1998.700962.
[239] M. S. McBeth and R. F. Jones, "A compact interferometric radar for studying clear air turbulence," in *Proc. IEEE Radar Conf.*, 2017, pp. 233–237, doi: 10.1109/RADAR.2017.7944203.
[240] T. Ohira, "A battery-less electric roadway vehicle runs for the first time in the world," in *Proc. IEEE Microw. Theory Technol. Soc. Int. Conf. Microw. Intell. Mobility*, 2017, pp. 75–78, doi: 10.1109/ICMIM.2017.7918860.

RONNIE S. SIEGEL received the B.A. degree in natural science and fine arts from Colgate University, Hamilton, NY, USA, and the M.LA. (master's degree in landscape architecture) from the University of Pennsylvania, Philadelphia, PA, USA. She is a licensed landscape architect and worked in New York, Virginia, and California designing public parks, playgrounds, school campuses, and residential projects as the Principal of Swire Siegel, Landscape Architects. She has promoted the use of native plants, conservation of water, and storm water recharge in her landscape architectural projects in Southern California and has served on local governmental committees to promote water conservation. Her architectural work has focused on the design of nature-based play environments for children in urban areas. She has promoted the benefits of open space design for children as a Guest Lecturer for the World Forum on Nature Education in Nebraska and for similar conferences around the world. In addition, she created a Global Interactive Art Project called *Carry the EARTH*, which collected stories from around the world from 2018 to 2023. She has written and illustrated a fictional children's book *DISPLACED: A Story About Climate Change and How Displaced Animals Ring the Alarm*. She is actively promoting climate action within her professional organization, the American Society of Landscape Architects. In 2021 she developed and implemented a speaker series that paired senior scientists and their research with well known landscape architectural firms and principals whose projects put this research into practice. She has created informational webinars, and is preparing a nature-based solutions track in the USGBC-LA's climate conference in 2024. As a Member of the ASLA Climate Action Committee, she is helping to prepare resources to help landscape architects across the country better address climate change mitigation and adaptation in their work. She is uniquely placed and very interested in bringing together scientists and practitioners that will help solve our growing climate change concerns.

PETER H. SIEGEL (Life Fellow, IEEE) received the B.A. degree in astronomy from Colgate University, Hamilton, NY, USA, in 1976, and the M.S. degree in physics and the Ph.D. degree in electrical engineering (EE) from Columbia University, New York City, NY, in 1978 and 1983, respectively. He has held appointments as a Research Fellow and Engineering Staff with the NASA Goddard Institute for Space Studies, New York City, from 1975 to 1983; a Staff Scientist with the National Radio Astronomy Observatory, Central Development Labs, Charlottesville, VA, USA, from 1984 to 1986; a Technical Group Supervisor and Senior Research Scientist with the Jet Propulsion Laboratory (JPL), National Aeronautics and Space Administration (NASA), Pasadena, CA, USA, from 1987 to 2014; and a Faculty Associate in electrical engineering and Senior Scientist in biology with the California Institute of Technology (Caltech), Pasadena, CA, USA, from 2002 to 2014. At JPL, he founded and led for 25 years, the Submillimeter Wave Advanced Technology Team, a group of more than 20 scientists and engineers developing THz technology for NASA's near and long-term space missions. This included delivering key components for four major satellite missions and leading more than 75 smaller research and development programs for NASA and the U.S. Department of Defense. At Caltech, he was involved in new biological and medical applications of THz, especially low-power effects on neurons and most recently millimeter-wave monitoring of blood chemistry. He was an IEEE Distinguished Lecturer and the Vice-Chair and Chair of the IEEE MTTS THz Technology Committee. He is currently an elected Member of the MTTS AdCom. He has more than 300 articles on THz components and technology and has given more than 250 invited talks on this subject throughout his career of 45 years in THz. His current appointments include the CEO of THz Global, a small research and development company specializing in RF bio-applications, a Senior Scientist Emeritus of biology and electrical engineering with Caltech, and a Senior Research Scientist Emeritus and a Principal Engineer with the NASA Jet Propulsion Laboratory. Dr. Siegel has been recognized with 75 NASA technology awards, ten NASA team awards, NASA Space Act Award, three individual JPL awards for technical excellence, four JPL team awards, and IEEE MTTS Applications Award in 2018. He is honored to continue the responsibilities in 2022, as the Founding Editor-in-Chief of IEEE JOURNAL OF MICROWAVES, which he hopes will invigorate the microwave field. Among many other functions, he was the Founding Editor-in-Chief for IEEE TRANSACTIONS ON TERAHERTZ SCIENCE AND TECHNOLOGY, from 2010 to 2015, and the Founder, in 2009, Chair through 2011, and has been elected General Secretary since 2012, of the International Society of Infrared, Millimeter, and Terahertz Waves (IRMMW-THz), the world's largest non-profit society devoted to THz science and technology. Dr. Siegel is also an appointed Editorial Board Member of IEEE ACCESS through 2025.